Development of a Holocene glacier-fed composite alluvial fan based on surface exposure-age dating techniques: the Illåe fan, Jotunheimen, Norway

Lindsey J. McEwen, John A. Matthews and Geraint Owen

1. Introduction

Alluvial fans are low-angle, fan-shaped depositional landforms created where a steep, sediment-laden stream channel, downstream of an upland sediment source, debouches onto a flatter surface, leading to a reduction in stream power (Parker *et al.*, 1998; Harvey, 2004, 2013; Harvey et al., 2005; Bowman, 2019). As products of the interactions between hydrological and sedimentological processes, alluvial fans can represent valuable sedimentary archives of fluvial adjustment to environmental change based on changing flow patterns and sediment transport regimes (Harvey et al., 2012; Stock, 2013).

Research into the dynamics and evolution of alluvial fans has involved a variety of approaches using conceptual models, field experiments, monitoring programmes, physical and numerical models, high-resolution morphometric analyses, palaeoenvironmental reconstruction and climate change scenarios (de Moor and Verstraeten, 2008; Giles et al., 2010; Scheinert et al., 2012; Støren and Paasche, 2014). When unravelling the development of alluvial fans, establishing a timescale for changing sediment inputs is critical, and dating techniques are essential to capture this history. The calibrated- (absolute) and relative-age dating techniques that have been applied in the context of the evolution of alluvial fans have been recently summarised by Bowman (2019), and reviewed in detail by Schneuwly-Bollschweiler et al. (2013). Historical analysis (D'Agustino, 2013), lichenometry (Jomelli, 2013), dendrochronology (Stoffel, 2013), radiocarbon dating (Chiverrell and Jakob, 2013), luminescence dating (Lang, 2013) and cosmogenic nuclides (Ivy-Ochs et al., 2013) have all been successfully applied over decadal to millennial timescales. However, the relatively new technique of Schmidt-hammer exposure-age dating (SHD) (e.g. Matthews and Owen, 2010; Shakesby et al., 2011; Stahl et al., 2013; Matthews et al., 2015; 2018; Tomkins et al., 2016, 2018; Wilson and Matthews, 2016; Winkler et al., 2016; Wilson et al., 2017, 2019) has yet to be applied in the context of alluvial fans, despite being eminently suitable for establishing the exposure age of surface boulders.

While the development and response of alluvial fans to environmental changes have been widely studied in temperate, semi-arid and cold environments (e.g. Bull, 1977; Rachocki and Church, 1990; Harvey, 2004, Harvey et al., 2005; Kjaer et al., 2004; Poulos and Pierce, 2018; Ventra and Clarke, 2018), examples from different types of glacially-fed alpine settings are lesser represented in research. Several studies on fan development in the Europeans Alps, a temperate high mountain setting, focus on debris flow fans and different fan morphologies, including their classification (see Crosta and Frattini, 2014; Jarman et al., 2011; De Haas et al., 2018). These fans would not necessarily be called 'alluvial' due to their (partial) development by non-fluvial processes such as debris flows. McEwen et al. (2011) provide one of few studies of an alluvial fan in a glacially-fed alpine setting, finding that the fan in Langedalen, southern Norway, was predominantly formed during and since the Little Ice Age cold period. In this case, the snout of a valley glacier extended onto the fan apex during the Little Ice Age maximum (ca. AD 1750), explaining the rapid increases in sediment supply and large-scale fan aggradation. The variable development of glacier-fed alluvial fans therefore requires further investigation. Barnard et al. (2006), studying fans and terraces in glacierized Himalayan catchments, suggest that Late Quaternary and Holocene fan and terrace formation and sediment transfer are linked to temporal changes in discharge and sediment load caused by glacier oscillations responding to climate change.

Sedimentary stratigraphy and architecture within fans may capture aspects of the responses to glacial fluctuations linked to climate and other environmental changes (e.g. Hornung et al., 2010; Brisset et al., 2014). However, reconstructions based on this approach are often incomplete due to the complexity of many fans formed over long timescales, and the difficulties of accessing and dating the subsurface. An alternative approach is taken in this paper, based on the dating of surface landforms. This approach has been possible in a case study of the Illåe fan in Leirdalen, Jotunheimen, southern Norway, which is a relatively simple, glacier-fed alluvial fan that developed over a relatively short timespan, entirely within the Holocene. Our specific objectives are:

- To describe the geomorphology of this fan;
- To identify and date, using several techniques, the different phases of fan development;
- To apply, for the first time, SHD in the context of alluvial fans;
- To infer and evaluate the dynamics of fan development with particular reference to flow types, sediment supply and the effects of glaciers;
- To compare the Illåe fan with other glacier-fed fans in the region;
- To propose a general conceptual model of fan evolution for alpine glacierized catchments related to Holocene environmental change.

2. Environmental setting and climate history

The Ytre Illåe, a major tributary of the Leira, in central Jotunheimen, has a catchment area of 22.65 km^2, of which 38% is glacierized (Fig. 1; see also Andreassen and Winsvold (2012). The Illåe fan has been formed by the Ytre Illåe, downstream of the confluence of the Nordre (North) Illåe and Søre (South) Illåe rivers, which are fed by the glaciers Nordre and Søre Illåbrean and two smaller unnamed glaciers.

The fan lies at an altitude of 1000-1100 m a.s.l., close to the present day birch (*Betula pubescens*) tree line, which is located at about 1200 m a.s.l. on the eastern hillslope of lower Leirdalen but has been depressed in the vicinity of the fan by grazing animals, especially goats, in recent centuries. Low-alpine vegetation (dwarf-shrub and lichen heath) characterises the surface of the present-day fan (NIJOS, 1991; Moen, 1999). Based on climatic data from the Sognefjell meteorological station (1413 m a.s.l.), mean annual air temperature is about +5.0 °C and mean annual precipitation is about 1000 mm on the fan (Aune, 1993; Førland, 1993). The geology of the area consists primarily of pyroxene-granulite gneiss with peridotite intrusions and quartzitic veins (Battey and McRitchie, 1973; Lutro and Tveten, 1996).

Deglaciation of Leirdalen occurred late in the Preboreal chronozone of the early Holocene. Radiocarbon-dated peat deposits in lower Leirdalen indicate deglaciation shortly before ~10,100 cal a BP (Barnett et al., 2001), while radiocarbon-dated birch (*Betula pubescens*) wood from upper Leirdalen indicates deglaciation there shortly before ~9,700 cal a BP (Matthews et al., 2005). These local minimum estimates of the date of deglaciation are consistent with large-scale modelling of the pattern and timing of deglaciation of the Scandinavian Ice Sheet following the Younger Dryas in southern Norway (Hughes et al., 2016; Stroeven et al., 2016). It is assumed, therefore, that deglaciation of the area occupied by the Illåe fan occurred shortly before the younger of two glacier re-advances of the Erdalen Event, which has been dated elsewhere in southern Norway to ~9.7 ka (Dahl et al., 2002).

Scots pine (*Pinus sylvestris*) migrated into Leirdalen by ~9.8 ka replacing vegetation dominated initially by birch (Barnett et al., 2001). During the early-Holocene thermal maximum, therefore, trees are likely to have completely covered the fan surface, affecting its hydrological regime, sediment supply and potential stability. At that time, the local glaciers were much reduced in size and, at least from 7.5-6.0 ka, melted away completely (Matthews and Dresser, 2008). Late-Holocene climatic deterioration resulted in downward migration of the tree line in Leirdalen while neoglaciation from ~5.5 ka culminated in the 'Little Ice Age' glacier maximum of the mid-eighteenth century (Matthews, 1974, 2005). The extent of latero-terminal moraines fronting the present-day glaciers (Fig. 1) indicates a glacierized area of 45 % at that time. Superimposed on these general trends, seven centennial- to millennial-scale glacier variations ('neoglacial events') have been identified in the neighbouring Smørstabbtindan massif (Matthews and Dresser, 2008), which would also have affected the extent of the Nordre and Søre Illåbrean glaciers, the hydrology of the Ytre Illåe river, and sediment supply to the fan.

There is limited historic information about extreme floods on the Illåe. However, in reconstructing flood histories in Leirdalen and downstream Bøverdalen from archival and data sources, McEwen and Matthews (2013) identified a series of extreme floods during the Little Ice Age, generated by extreme rainfall. These included events in AD 1655 (Roald, pers. comm.), 1743 (Grove and Battagel, 1989), 1789 (known as 'Storofsen'; Roald, 2003) and 1860 (Roald, 2000). The event in July 1789 is known to have caused significant erosion in Bøverdalen (Roald, pers. comm.). More recently, a large localised flood occurred on the Illåe in May 2004 (personal observation).

3. Methods

An integrated, multi-proxy research design was used to characterise and date the development of the fan. Morphological features, including prominent boulder deposits on the upper fan surface, the area affected by river entrenchment and an associated terrace sequence, were mapped onto aerial photographs dating from 2004, 2010 and 2017 (Fig. 2). SHD, lichenometric dating, soil development and soil radiocarbon dating were used to provide numerical ages and/or relative-age assessments for the upper fan surface and the terraces. Observations were made of sub-surface sediment composition and stratigraphy at a limited number of exposures within the entrenched section of the fan. The form and measured clast characteristics of the boulder deposits were used as the main criteria to determine the nature of the flows responsible for fan development, and to infer the competence and hence relative magnitude of the flows that generated the boulder deposits on different zones on the fan surface.

Numerical age estimates of the boulder deposits on the upper fan surface were obtained using SHD, supplemented by lichenometry and a single terrestrial cosmogenic-nuclide date (TCND). For application of SHD, the fan surface was divided into eight sampling zones where the boulder deposits were most extensive (Fig. 2). SHD was used primarily to date boulder deposits on the upper surface of the fan; there were insufficient exposed boulders on the incised terraces to enable the use of SHD there. We used high-precision Schmidt-hammer exposure-age dating, following closely the approach developed by Matthews and Owen (2010), Matthews and Winkler (2011) and Matthews and McEwen (2013). This involves a linear calibration equation, which relates Schmidt-hammer R-values to 'old' and 'young' control points (surfaces of known age) and the calculation of 95% confidence intervals for age, which combine the calibration error (C_t) associated with the calibration equation with the sampling error (C_s) associated with the surface to be dated. The 'South and East Smørstabbtindan' calibration curve of Matthews and Owen (2010) was used to obtain age estimates for the boulder deposits within each zone of the upper fan surface. This curve is based on local control points from glacially scoured, pyroxene-granulite bedrock surfaces of known age from Leirdalen and Gravdalen, and is therefore considered highly appropriate for boulders of similar lithology in the boulder deposits.

A standard mechanical type-N Schmidt hammer (Proceq, 2004) was used on near-horizontal boulder surfaces associated with the extensive boulder deposits on the fan surface. Unstable boulders, edges and cracks, lichen thalli, wet surfaces and unusual lithologies (in this case, peridotite and quartz) were avoided and a test anvil was used before and after use to ensure that there was no deterioration in the Schmidt hammer (cf. McCarroll, 1987; 1994). Within each of the eight zones on the upper surface of the fan (Fig. 2), 750 Schmidt-hammer impacts (R-values) were recorded in 30 sub-locations (i.e. one impact per boulder; 25 boulders from each sub-location). Use of a large number of sub-locations ensured R-values were representative of the boulder deposits spread across each zone. Use of a single impact from each boulder ensured that the frequency distribution of R-values is equivalent to the age-distribution of boulders (Matthews et al., 2015). Care was taken to avoid boulders on terrace margins in case they might have tumbled from a higher level. The mean R-value and its 95% confidence interval for each of the eight zones of the fan were calculated from 30 site-mean R-values (i.e. n = 30 sites).

Lichenometric dating was undertaken separately for boulder deposits of the northern and southern parts of the upper fan surface, for the south-side terrace sequence (Fig 2), and for two terraces that could be recognised on the south-side. The long axes (maximum diameter) of the five largest lichens of the yellow-green, crustose *Rhizocarpon* subgenus were measured (cf. Matthews, 1974; 2005). The 'Central Jotunheimen' lichenometric dating curve based on the mean of the five largest lichens (Matthews, 2005) was used to provide minimum estimates of exposure age, and hence time elapsed since deposition of the boulder deposits. This local growth curve is based on control points (surfaces of known age) using historically-dated moraines from neighbouring glacier forelands. Limitations of these curves in their application to fluvial environments are considered by McEwen and Matthews (2013). Little previous assessment has been made as to how reliably such curves can be transferred to fluvial deposits with potentially different and variable moisture and snow-cover characteristics. Limited information also exists about the tolerance of *Rhizocarpon* species to flood inundation, and associated corrosion by bedload, siltation and episodic burial. In the present application, the lichenometric results from the terraces must be treated with caution for the additional reason that some of the terrace surfaces have relatively few cobbles and boulders suitable for lichen colonisation.

TCND (Cockburn and Summerfield, 2004; Dunai, 2010; Balco, 2011) was carried out primarily to provide an independent check on the SHD age estimates from the boulder deposits on the upper fan surface. This was based on ^{10}Be from a quartz sample collected from an *in situ* boulder in zone 5 (site X in Fig. 2; see also Fig. 3). Sample preparation and measurement followed the procedures of Child et al. (2000) and the Lal/Stone ^{10}Be production rate scaling scheme was employed (Lal, 1991; Stone 2000). Further details of this are given in Matthews et al. (2007). Radiocarbon dating was carried out on the acid-washed fraction of the soil organic matter, with the aim of obtaining minimum ages for the upper surface of the fan and the terrace surfaces, following procedures detailed in Matthews (1985).

Analysis of the boulder deposits was carried out within each of the zones previously established for SHD. Sediment calibre was measured using the intermediate (b-axis) of the 50 largest clasts, from which representative clast sizes (D_{50}, D_{84} and maximum clast size) were calculated (Brierley and Hickin, 1985; Bunte and Abt, 2001). Powers (1953) roundness index was measured for

50 clasts and used to calculate a mean roundness index to interpret the likely sediment sources and depositional processes. Palaeohydrological parameters associated with the flows that deposited the sediment in the boulder deposits were estimated from the maximum intermediate-axis clast size (*d*) (Williams, 1983):

For unit stream power (ω) = $0.079\ d^{1.3}$ ($10 \leq d \leq 1500$ mm) (1)

For bed shear stress (τ) = $0.17\ d^{1.0}$ ($10 \leq d \leq 3300$ mm) (2)

For mean flow velocity (V) = $0.065\ d^{0.50}$ ($10 \leq \mathrm{d} \leq 1500$mm) (3)

4. Results

4.1 Morphology of the fan

The geomorphological map (Fig. 2) shows the distinctive features of the fan including the active zone close to the Ytre Illåe, which is entrenched into the extensive upper fan surface and within which the Ytre Illåe flows in a bedrock channel. The associated inset fan drains north-westwards towards the confluence of the Ytre Illåe with the Leira. Within the entrenched zone, a relatively narrow area of terracing is best developed south of the active zone (Fig. 4). The Ytre Illåe debouches from a substantial bedrock gorge, which extends upstream for about 1 km to the confluence of the Nordre and Søre Illåe. Most of the upper fan surface is covered with boulder deposits separated by relict channels which bifurcate and radiate from the fan apex. For reasons provided below, the entire fan is referred to as the 'Holocene fan' (~0.38 km^2) and the entrenched zone, including the terraces, with the inset fan as the 'late-Holocene fan' (~0.09 km^2).

A suite of four well-developed terraces is incised into the upper surface of the fan on the south side of the Ytre Illåe (Fig. 4). Here, the slopes of the upper fan surface and terrace 1 are 15%, while the lesser slopes of terraces 2-4 are within the range 7-8%. The inset fan is characterised by a relatively small active area of fresh unvegetated sediment deposition and recently abandoned channels around older, larger calibre deposits that act as keystones focusing later deposition. The slope of the inset fan is 5%, considerably less than that of the upper fan surface.

4.2 Morphology and composition of the boulder deposits

The typical form of the boulder deposits on the upper fan surface is a longitudinal, sometimes slightly sinuous, ridge, standing typically about 1 m above the intervening shallow channels (see Fig. 5 A-D). These elongate boulder deposits, which are up to ~100 m long and ~15 m wide, are extensive on both north- and south-sides of the fan, and continue to its lateral margins. However, they are notably absent within 200 m of the fan apex, where boulders have a more scattered distribution over the surface. In places, there is a high concentration of boulders at the downslope end of the ridge, which is lobe-like. However, in exposed sections along the margins of the inset fan, the ridges and boulder concentrations appear to be matrix-rich. Well-developed lobes are uncommon on the fan surface and there is no evidence of levées. Some of the intervening shallow channels have been modified by erosion, indicated by a step-like long-profile, with deeper erosion down-slope (below the step), but there is no sign of a braided system of channels or channels capable of supporting bars >1 m high.

4.3 Clast size, palaeohydrological indices and clast roundness in the boulder deposits

The calibre of the clasts in the boulder deposits ranges from a maximum b-axis (D_{max}) of 0.75 m (zone 5a) to 3.20 m (zones 2/4), and a median b-axis (D_{50}) of 0.38 m (zone 5) to 0.96 m (zone 3) (Table 1 and Fig. 6A). The clast size of sediment in a deposit reflects both the calibre of sediment available upstream for reworking and differential stream powers during flows. Minimum boulder-transport conditions for the largest boulder in deposits in each zone are estimated in Table 1. On the upper fan surface, lowest unit stream power for entrainment (ω) ranges from 432 Wm^2 (zone 5) to >2000 Wm^2 (zones 2-4 (south-side) and zone 6 (north-side). Four zones (2/3/4/6) have the largest clasts in their deposits that would have required significantly higher lowest unit stream powers for entrainment beyond the upper range of clast sizes used by Williams (1983). Lowest bed shear stresses for clast entrainment (τ) ranged from 128 to 544 Nm^{-2}. Values for both ω and τ are substantially lower for the sites on the inset fan and active zone than for most sites on the upper fan surface, indicating that much greater flows were involved in transporting and depositing boulders to the latter sites.

The mean roundness index varies little across all eight zones (Fig. 6B) and the overall average roundness is 4.05 with a standard deviation of 0.14, which indicates a strong subrounded modal class. The average for all zones is closely comparable to the mean roundness of 4.06 for the inset fan. Minimum roundness values of 3.78 and 3.80 characterise deposits in zones 1 and 6, respectively, both near the fan apex (south- and north-side, respectively). Maximum roundness of 4.20 is recorded from zone 4, which is comparable to, but slightly higher than, that of the inset fan. These clast roundness values are interpreted as reflecting the small catchment, which has a significant glacierized area and limited distance for abrasion by fluvial or any other flow processes.

4.4 Fan stratigraphy

Sections through the fan deposits are exposed on the north and south banks of the active channel (Fig. 7. A-D). A synthetic stratigraphy has been constructed, which adheres most closely to sections on the south bank where the maximum thickness of sediments reaches 18 m (Fig. 8). The deposits comprise boulders up to approximately 1.5 m maximum diameter interbedded with gravel-rich fines. The ratio of boulders to fines is very variable, and these variations pick out a crude stratification in places (see Fig. 7A and C). Boulder-rich intervals are 1-2 m thick, but lateral continuity was not clear due to slumping of material. Some of these intervals are clast-supported while others are matrix-supported. In some sections on the north side, similar boulder-rich intervals form clast-supported lenses of the order of 20 m in length. The intervening intervals form crude beds up to 6 m thick that fine upwards from matrix-supported, boulder-rich bases. Clast-supported, boulder-rich layers or lenses occur at several levels in the sections, suggesting that the boulder deposits, like those evident on the fan surface, are present throughout the fan thickness and are not just a feature of the present-day fan surface. A limited number of boulder-rich intervals suggest, moreover, that fan aggradation was achieved through a limited number of major depositional events.

4.5 Dating the boulder deposits

Mean R-values for boulders within deposits on the upper fan surface are highly consistent, ranging from 44.01 ± 0.92 to 47.15 ± 1.00 for the eight zones (Table 2). The average R-value across the eight localities is 45.13 ± 1.02. SHD ages (rounded to the nearest 5 years) are correspondingly consistent: all zones are of similar age, within the range 7080 ± 450 to 8220 ± 440 years. These results demonstrate that the upper surface of the fan has been inactive for at least the last 7000 years, which is confirmed by an age of 7820 ± 300 years when the data from all areas of the fan are included in a single SHD age estimate. The fact that zone 1 yielded the youngest age is consistent with the fan apex being active for up to ~1000 years longer than the remainder of the fan, which can be interpreted as having been inactive for ~8000 years.

The SHD dating is corroborated by the TCND age of the sample collected from a boulder deposit in zone 5, which yielded an estimated age of 6075 ± 1220 years (± 2σ). However, in the light of the wide confidence interval and the SHD results, this TCND age is likely to be an underestimate of the true age of the upper fan surface by at least ~1000 years.

Lichen sizes of >300 mm are common on the boulder deposits, suggesting minimum ages for the upper fan surface (on both the north- and south-sides) of the order of 2000 years. These results should not be interpreted as close minimum age estimates, however, because they are extrapolations far beyond the range of the lichenometric dating curve, and also exceed the likely longevity of lichens of the *Rhizocarpon* subgenus in southern Norway (cf. Innes, 1985a; Matthews and Trenbirth, 2011). Using the same lichenometric dating curve, the predicted age of the single largest lichen from the boulder deposits is ~4600 years. However, this must also be regarded as an unrealistic estimate of the true age of the upper fan surface.

4.6. Dating the terrace sequence

Importantly, the largest lichens on terrace 1 (maximum diameters of 365 and 330 mm to the south and north of the Ytre Illåe, respectively) are broadly comparable in size to those on the upper fan surface (Table 3). Mean diameters on this terrace are significantly smaller, however, which suggests an age of the order of ~1000 years. Because of the aforementioned limitations of lichenometric dating in this context, these lichenometric results must again be regarded as providing large underestimates and therefore unreliable estimates of true terrace age.

Lichen sizes of <165 and <112 mm and lichenometric ages of 149 and 179 years for south-side terraces 2 and 3, respectively, are much more likely to reflect true terrace age because they are the result of interpolation (rather than extrapolation) of the lichenometric dating curve. The results from north-side terrace 2 and the surface of the inset fan, with largest lichens of ~200 mm and predicted ages of 432 and 474 years, respectively, suggest that the oldest parts of these landforms may have last been active early in the Little Ice Age period (cf. Matthews and Briffa, 2005). South-side terrace 4, where a lichenometric age of <100 years is indicated, is likely to have been formed by a flood in historical times, some of which have been documented (McEwen and Matthews, 2013).

Soils on the terrace surfaces (Fig. 9), which can be classified as alpine Brown Soils (Ellis, 1979, 1980), are characterised by a thin uppermost organic-rich (A_o) horizon, dark brown to orange, predominantly mineral (A/B) horizons of variable thickness overlying the subsoil (C horizon). South-side profiles can be interpreted as a developmental sequence or chronosequence on the basis of soil depth and horizon thickness: terrace 1 has the most developed profile, while the soil on terrace 4 is clearly embryonic. The profile from the upper fan surface (south-side), which was located closely adjacent to the south-side terrace profiles, appears anomalously thin, which may be accounted for by long-term deflation in its exposed position. Soils from the north-side are more complex, with textural variations, including silt-rich layers (s), which are interpreted as aeolian, slope-wash and/or fluvial deposits, which interrupted soil development and, in places, created buried paleosols (p).

Radiocarbon dates from organic material in predominantly minerogenic horizons yield minimum estimates of the age of the soil and land surface on which the soil has developed (Matthews, 1985). The oldest date from the upper fan surface (north-side) is no more than ~2000 years, while those from the other profiles, including those from the terraces are all less than ~1000 years (Table 4). These radiocarbon dates clearly do not reflect the true ages of either the upper fan surface or the terraces (with the possible exception of terrace 3 (south-side), as further elaborated in the discussion. Problems with dating soil organic matter, such as low carbon content, high carbon turnover and low apparent residence times in well-drained soils, and contamination by young root penetration, provide likely explanations for such underestimates of land-surface age (cf. Matthews, 1985).

5. Discussion

5.1. Nature of the boulder deposits and flow processes

Alluvial fans are typically classified into those dominated by stream flow (water floods) and those dominated by debris flow (gravity flows) (Rachocki and Church, 1990; Harvey et al., 2005, Harvey, 2013; Bowman, 2019). The former tend to be much larger than the Illåe fan, with a low-angle surface characterised by braided channels and well-sorted sedimentary deposits. In contrast, the latter tend to be small in area and associated with small, rugged catchments in mountains and uplands, and their surface slopes are steeper with levées and lobes composed of unsorted diamictons (Harvey, 2004; Ventra and Clarke, 2018). The distinctive morphologies of these two types of fans are the product of the distinctive flow processes which, in turn, stem from much higher debris concentrations in debris flows than in water floods.

At first sight, the morphology and basin characteristics of the Illåe fan might appear to match those of the debris-flow type. Indeed, the surface boulder deposits on this and similar fans have been classified previously as debris-flow lobes (Innes, 1985b, 1985c). However, close examination of the landforms and sediments associated with the Illåe fan indicate they are not typical of debris-flow fans or debris-flow processes. Debris-flow levées are absent and the elongate boulder deposits rarely have a lobate form. We are therefore able to rule out the possibility that the boulder deposits are debris-flow deposits, and argue below that they are the product of debris floods, characterised by hyperconcentrated flows (i.e. flows with a higher debris concentration than stream flows and a lower debris concentration than debris flows). There is increasing recognition of such intermediate-type flows which, although relatively poorly understood, would be expected to be associated with intermediate-type landforms and sedimentary deposits (cf. Costa, 1984; Wells and Harvey, 1987; Hungr et al., 2001; Wilford et al., 2004; Pierson, 2005; Harvey, 2013; Germain and Ouellet, 2014; Calhoun and Clague, 2018).

Lack of boulder deposits close to the fan apex indicates very energetic transport of water and sediment from the rock-cut gorge upstream. Longitudinal boulder ridges formed lower down the fan where the energy level dropped and greater deposition occurred. However, similar boulder deposits continue to the fan margin and Leira river, indicating rather fluid flows with high debris concentration, consistent with hyperconcentrated flow. Matrix-supported material dominating the fan stratigraphy rules out simple fluvial processes. The modification by erosion of some shallow troughs on the fan surface shows that generally non-erosive water flow was later focussed along the troughs and around the ridges, ruling out the possibility that the lobes represent bars within a channel system.

The large areal extent of the Illåe fan masks a relatively shallow thickness of sediment (as revealed by down-cutting of the Ytre Illåe to bedrock). In the stratigraphy, the boulder concentrations in the sections are interpreted as cross-sections of longitudinal ridges, while a limited number of distinct intervals of clast-supported sediment rich in boulders indicate that the boulder deposits on the fan surface do not represent a unique late phase of fan development. Boulder size in the deposits on the upper fan, inconclusive evidence of imbrication and the minimum thresholds of entrainment indicate deposition by relatively large debris floods with a large volume of high-calibre bedload beyond the competence of the modern flow regime. While all boulders have clearly been transported during these debris floods, the slightly higher proportion of more angular boulders on the upper fan may relate to a greater proportion of angular material of frost-shattered origin flushed from the gorge (McEwen et al., 2002).

5.2. Early-Holocene (paraglacial) fan aggradation

When were the boulder deposits and the underlying fan sediments deposited, and what causal factors led to boulder concentrations high enough to produce the debris floods? The SHD ages, corroborated by the TCND date, are of direct relevance to the first part of this question. They allow the identification of the earliest phase of fan development, and provide relatively accurate age estimates for stabilisation of the upper fan surface. Our extensive SHD results indicate that the boulder deposits and the whole of the upper fan surface had been deposited and stabilized by ~8000 years ago. This, in turn, indicates that the majority of the sediment stored in the fan was deposited within ~2000 years of deglaciation and therefore that the fan is essentially a relict paraglacial landform (Church and Ryder, 1972; Ballantyne, 2002; Mercier, 2008), conditioned by former glaciation.

Several factors would have contributed to this paraglacial phase of fan development, which was characterised by fan aggradation beginning with deglaciation c. 9.7 ka and more-or-less ending by 8.0 ka. First, a till-mantled catchment with initially low vegetation cover would have been highly susceptible to fluvial and gully erosion and reworking by rapid mass movements in feeder gullies within the paraglacial sediment cascade (cf Ballantyne, 2003; Mercier, 2008). During deglaciation, the whole landscape would have become susceptible to erosion, especially during high-magnitude floods. Second, an initially highly glacierized area would have contributed to relatively high discharges, flows with high debris concentrations, and high-calibre bedload. Third, as the early-Holocene ice sheet reduced in size and vegetation cover increasingly stabilised the landscape, the till sources would have become increasingly unavailable, and sediment supply to the fan surface would have reduced. The high proportion of subrounded boulders characteristic of the boulder deposits provides evidence not only of abrasional transport but also of a predominant till source. Slightly more angular material on the upper fan may be explained by this material being deposited just before the fan stabilised when paraglacial till sources were dwindling. At this time, angular material from the gorge may have increased in proportion to the till source (cf. McEwen et al., 2002).

5.3. Mid-Holocene fan stability

Whereas the stabilization of the upper fan surface has been dated to within a millennium by exposure-age dating, the duration of the stable phase is very poorly constrained by the soil radiocarbon dates. Fan stability is likely to have persisted through a long interval of the mid Holocene when, from ~8.0 to 5.5 ka, glaciers both in the neighbouring Smørstabbtindan massif and more widely throughout southern Norway were smaller than today and absent for much of the time (Matthews and Dresser, 2008; Nesje, 2009). This period of time corresponds with the Holocene Thermal Maximum (HTM) when, according to local and regional proxy records, mean annual air temperature is likely to have been 1.0-3.0 °C higher than today (Dahl and Nesje, 1996; Jansen et al., 2008; Seppä et al., 2009; Velle et al., 2010; Lilleøren et al. 2012; Eldevik et al., 2014). As a consequence of the absence of glaciers in the catchment, higher evaporation rates and lower precipitation for much of this time interval, discharge and particularly bedload would have been correspondingly reduced. At the same time, stability of the fan would have been enhanced by the forest cover of pine and/or birch (Barnett et al., 2001; cf. Wilford et al., 2005). We envisage a largely non-erosive hydrological regime dominated by stream flow and water floods rather than debris floods.

5.4. Late-Holocene entrenchment and terrace development

Entrenchment of the Ytre Illåe brought this benign regime to an end, heralding terrace formation and deposition of the distal inset fan. The depth of soil and extent of horizon development on the terraces, the radiocarbon-dated soil material from the terraces, and the results of lichenometric dating, establish that most of the terraces pre-date the Little Ice Age, when local glaciers attained their late-Holocene maximum extent (Matthews, 1991; Matthews and Dresser, 2008). Lichenometric dating was useful, moreover, on the inset fan in clarifying the limited spatial extent of fan reworking by floods during the last few hundred years of the Little Ice Age.

Incision of the Ytre Illåe into the fan surface is likely to have been a response to neoglaciation – the late-Holocene recrudescence and growth of glaciers – which began ~5.0 ka (Matthews and Dresser, 2008). During neoglaciation, discharge would have increased but, as the glaciers occupied a very small area of the catchment, it is unlikely that the sediment load increased appreciably, at least initially. Thus, degradation rather than aggradation characterized that part of the fan into which the Ytre Illåe became incised. Downcutting by the Ytre Illåe may have been affected by century- to millennial-scale glacier and climatic variations during the late Holocene (cf. Matthews and Dresser, 2008), but our dating of the four terraces has not been sufficiently accurate to enable specific correlation with these. The terrace sequence nevertheless reflects the relatively small-scale adjustments that affected the hydrological regime sufficiently to produce phases of renewed downcutting.

5.5. Conceptual model of alpine alluvial fan evolution in relation to glaciers and Holocene climate

Our reconstruction of the history of the Illåe fan permits clarification of the potential role of glaciers in the development of alluvial fans, and enables proposal of a generalized conceptual model of alluvial fan development in glacierized catchments. It is clear is that extreme debris floods dominated during the aggradation of the fan, that water floods have been effective in its later entrenchment, and that glaciers, or their absence, played a dominant role throughout the evolution of the fan. The large calibre of sediment transported and deposited during aggradation provides evidence of high flood competence during the paraglacial phase, that seems incompatible with the present-day hydrology. Jøkulhlaups during deglaciation provide a possible explanation for higher discharges but the SHD ages of the deposits suggest that the higher discharges would have had to have persisted for at least two millennia after deglaciation. As deglaciation was rapid following the Erdalen Event, it is unlikely that debris floods would have been generated by glacier meltwater alone. This suggests they were also a response to high discharges from snow meltwater and/or rainstorms between late spring and early autumn. Even during the Little Ice Age, frequent high-magnitude floods (cf. Støren and Paasche, 2014) carried out limited geomorphic work compared to the debris floods that affected the Illåe fan during the early Holocene (in terms of both calibre of load and spatial extent of reworking) on the inset fan. The calibre of sediment (D_{84} 0.29 m; D_{max} 0.90 m) reworked by the 2004 flood on the Illåe may act as an analogue for past events during the Little Ice Age – a far lesser flood event than those that occurred in the early Holocene.

Fig. 10 presents a schematic conceptual model of alpine fan evolution in glacierized catchments that encompasses three phases of fan development: (1) early-Holocene paraglacial fan aggradation after deglaciation; (2) mid-Holocene stabilisation of the surface; and (3) late Holocene neoglacial incision/entrenchment. Fan formation is initiated by deglaciation in the early Holocene (~9.7 ka) and the main paraglacial development of the fan occurs within ~2000 years, with extensive boulder deposition due to a combination of both high sediment availability and debris-flood competence. Sediment availability, which declines exponentially as paraglacial effects diminish, is proposed as the main reason for the cessation of sediment aggradation and stabilisation of the upper surface of the fan, but other possibilities are accommodated in the model, such as sediment accessibility or exhaustion, increased evapotranspiration, reduced flood magnitude or frequency, and stabilisation of the fan surface by vegetation. During the HTM, the fan surface remains stable with reduced stream flow, tree cover, and possibly almost non-erosive shallow stream channels due to the absence of glaciers in the catchment, lower discharges and much reduced stream loads. With the onset of neoglaciation (~5.5 ka), rising discharges accompanied by relatively low sediment availability lead to downcutting and entrenchment, leaving the upper fan surface with an SHD age derived from boulder deposits of ~8.0 ka. Limited terrace development during entrenchment is attributed to short-term (century- to millennial-scale) glacier and climatic fluctuations. It is envisaged that one of the small channels on the upper fan surface becomes sufficiently erosive to initiate entrenchment into the fan deposits, rendering the upper fan surface as totally relict.

Our model explains why the Illåe fan was very active in the early Holocene but has been largely inactive since. It can also be used to explain why this fan is largely a relict feature whereas other fans, such as the Nystølen fan, in the Jostedalsbrean region of southern Norway (Lewis and Birnie, 2001; McEwen et al., 2011) developed later. In effect, the validity of the model inferred from the Illåe fan can be tested against the independent evidence from the Nystølen fan.

Radiocarbon dating and lichenometry have established that surface of the Nystølen fan dates from the Little Ice Age period and remains very active today. The answer to this apparent paradox requires an explanation of why the Illåe fan is primarily a paraglacial landform that formed during and shortly after deglaciation, whereas the Nystølen fan is primarily a Little Ice Age feature. This major difference in alluvial fan evolution can be explained in terms of differences in the respective contributing catchments and, particularly in the proportions of the catchments glacierized at various times during the Holocene. Both catchments contain glaciers today, but the Illåe catchment contains much smaller glaciers and hence a much smaller proportion of the catchment area is glacierized (38 %). When Nordre and Søre Illåbrean and the other glaciers in the catchment reached their Little Ice Age maxima, the proportion glacierized reached 45%. In contrast, at its Little Ice Age maximum, Nystølsbrean had advanced onto the apex of the Nystølen fan and the glacierized proportion of the catchment reached 100%. Consequently, discharge and sediment supply at the Nystølen fan were much greater at its Little Ice Age maximum than at the Illåe fan, and remain so today. Contrasting conditions also pertained at the two sites during early-Holocene deglaciation: the Illåe catchment contained an extensive till cover ripe for paraglacial sediment activation, whereas Nystølsbrean retreated to reveal a smaller, relatively rocky catchment with a smaller potential for the generation of sediment for debris floods.

A similar set of conditions to those affecting the development of the Nystølen fan have affected the fan in front of Hurrbrean, on the opposite side of the Leira river to the Illåe fan (Fig. 2 H). Hurrbrean also advanced onto its alluvial fan in the Little Ice Age, when its catchment was 100 % glacierized (as evinced by the presence of Little Ice Age moraines). Today, the Hurrbrean alluvial fan is extremely active but exhibits no evidence of debris floods, only water floods affecting its surface. The absence of debris floods can again be attributed to insufficient sediment supply to generate hyperconcentrated flow. As at the Nystølen fan, the

Little Ice Age glacier foreland of Hurrbrean is not a major source of sediment for the glacial river. This second fan from Jotunheimen shows that closely adjacent fans can exhibit very different histories of development. Taken together, the evolution of the Illåe, Nystølen and Hurrbrean fans not only support the model but also demonstrate the different outcomes for fans primarily affected by *neoparaglacial* as opposed to *paraglacial* environmental conditions – the former referring to effects attributable to recent deglacierization of Little Ice Age glacier forelands rather than the effects of deglaciation at larger scales of space and time.

6. Conclusions

- Dating of various surface elements of the Illåe fan has led to a conceptual model of alpine alluvial fan evolution in glacierized catchments related to Holocene environmental change. The study also highlights the application and potential of high-precision Schmidt-hammer exposure-age dating (SHD) in alluvial fan environments alongside other dating methods.

- Extensive Schmidt-hammer exposure-age dating (SHD) of boulder deposits on the upper surface of the fan, supplemented by a single terrestrial cosmogenic-nuclide date (TCND), established that most of the fan had formed by ~8.0 ka, and hence that it is essentially a relict landform. Minimum age estimates based on lichenometric and soil radiocarbon dates of up to ~2.0 ka were obtained from an entrenched terrace sequence and inset fan, which occupy a small area of the total fan. These dates allowed the differentiation of early- and late-Holocene events, and the recognition of three phases of fan development: (1) early-Holocene aggradation, (2) mid-Holocene stability, and (3) a late-Holocene entrenchment.

- Local glacier history is inferred to have been the dominant control on the chronology of alluviation. Regional deglaciation by ~9.7 ka initiated the paraglacial phase of aggradation. This was a response to high sediment availability following deglaciation and an initially unvegetated catchment, subject to high-magnitude hyperconcentrated flows or debris floods. These intermediate-type flows produced extensive and distinctive transitional boulder deposits on the upper fan surface and account for most of the sediment deposited during the aggradation phase. The stable phase, which coincided with the HTM, when glaciers were absent from the catchment and the fan was tree covered, resulted largely from the reduced bedload. Entrenchment and terrace formation are seen as a response to the regrowth of glaciers during neoglaciation after ~5.5 ka, culminating in the Little Ice Age of recent centuries.

- Whereas Little Ice Age glacier expansion was relatively unimportant in fan development on the Illåe, the Nystølen fan in western Norway and the Hurrbrean fan in Jotunheimen grew extensively at that time, as a result of neoparaglacial aggradation following complete glacierization of their catchments. The contrasting development of these two fans provided a test and corroboration of our generalised conceptual model, and support for the association of the main early-Holocene aggradation phase of the Illåe fan with paraglacial debris floods.

Acknowledgements

Fieldwork was carried out on the Swansea University Jotunheimen Research Expeditions, 2007, 2010, 2011 and 2019. Radiocarbon dating of the soil samples was carried out in the Swansea Radiocarbon Dating Laboratory by P Quentin Dresser. Thanks are also due to Derek Fabel who carried out preparation of the rock sample and TCND dating at the Glasgow University – Scottish Universities Environmental Research Centre Cosmogenic Isotope Laboratory. We are also grateful to Richard Shakesby for facilitating the TCND dating, Lars Roald (NVE) for information on local flood history, and John Hiemstra and Amber Vater for assistance in the field. Anna Ratcliffe prepared several of the figures for publication. This paper represents Jotunheimen Research Expeditions, Contribution No. 213 (see http://jotunheimenresearch.wixsite.com/home).

References

Andreassen, L.M., Winsvold, H., 2012. Inventory of Norwegian glaciers. Norwegian Water Resources and Energy Directorate, Oslo.

Aune, B., 1993. Temperatur Normaler, Normalperiode 1961-1990. Den Norske Meterorologiske Institutt, Oslo (Rapport 02/93).

Balco, G., 2011. Contributions and unrealized potential contributions of cosmogenic-nuclide exposure dating to glacier chronology, 1990-2010. Quaternary Science Reviews 30, 3-27. https://doi.org/10.1016/j.quascirev.2010.11.003

Ballantyne, C.K., 2002. Paraglacial geomorphology. Quaternary Science Reviews 21, 1935-2017. https://doi.org/10.1016/S0277-3791(02)00005-7

Barnard, P.L., Owen, L.A., Finkel, R.C., 2006. Quaternary fans and terraces in the Khumbu Himal south of Mount Everest: their characteristics, age and formation. Journal of the Geological Society, London 163, 383-399. https://doi.org/10.1144/0016-764904-157

Barnett, C., Dumayne-Peaty, L., Matthews, J.A., 2001. Holocene climatic change and tree-line response in Leirdalen, central Jotunheimen, south central Norway. Review of Palaeobotany and Palynology 117, 119-137. https://doi.org/10.1016/S0034-6667(01)00081-1

Battey, M.H., McRitchie,W.D., 1973. A geological traverse across the pyroxene-granulites of Jotunheimen in the Norwegian Caledonides. Norsk Geologiske Tidsskrift 53, 237-265.

Bowman, D., 2019. Principles of Alluvial Fan Morphology. Springer, Dordrecht https://doi.org/10.1007/978-94-024-1558-2

Brierley G.J., Hickin E.J., 1985. The downstream gradation of particle sizes in the Squamish river, British Columbia. Earth Surface Process and Land¬forms 10, 597-606. https://doi.org/10.1002/esp.3290100607

Brisset, E, Miramont,C., Edward J., Anthony, E.J., Bruneton, H., Rosique, T., Sivan O., 2014. Sediment budget quantification of a sub-Alpine river catchment since the end of the last glaciation. Catena 114, 169-179. https://doi.org/10.1016/j.catena.2013.08.004

Bull, W.B., 1977. The alluvial fan environment. Progress in Physical Geography 1, 227-270. https://doi.org/10.1177/030913337700100202

Bunte K., Abt S.R. 2001. Sampling Surface and Subsurface Particle-size Distributions in Wadable Gravel- and Cobble-bed Streams for Analyses in Sediment Transport, Hydraulics, and Streambed Monitoring. General Technical Report RMRS-GTR-74, Fort Collins CO: U.S. Department of Agriculture, Forest Service, Rocky Mountain Research Station, 428 pp. https://doi.org/10.2737/RMRS-GTR-74

Calhoun, N.C., Clague, J.J., 2018. Distinguishing between debris flows and hyperconcentrated flows: an example from the eastern Swiss Alps. Earth Surface Processes and Landforms 43, 1280-1294. https://doi.org/10.1002/esp.4313

Child, D., Elliott, G., Mifsud, C., Smith, A.M., Fink, D., 2000. Sample preparation for earth science studies at ANTARES. Nuclear Instruments & Methods in Physics Research, Section B: Beam Interactions with Materials and Atoms 172, 856-860. https://doi.org/10.1016/S0168-583X(00)00198-1

Chiverrell, R., Jakob, M., 2013. Radiocarbon dating: alluvial fan/debris cone evolution and hazards. In Schneuwly-Bollschweiler, M., Stoffel, M., Rudolf-Miklau, F., (Eds.) Dating Torrential Processes on Fans and Cones. Springer, Dordrecht. pp. 265-282. https://doi.org/10.1007/978-94-007-4336-6_17

Church, M., Ryder, J.M., 1972. Paraglacial sedimentation: a consideration of fluvial processes conditioned by glaciation. Geological Society of America Bulletin 83, 3059-3072. https://doi.org/10.1130/0016-7606(1972)83[3059:PSACOF]2.0.CO;2

Cockburn, H.A.P., Summerfield, M.A., 2004. Geomorphological applications of cosmogenic isotope analysis. Progress in Physical Geography 28, 1-42. https://doi.org/10.1191/0309133304pp395oa

Costa, J.E., 1984. Physical geomorphology of debris flows. In Costa, J.E., Fleisher, P.J., (Eds.) Developments and Applications of Geomorphology. Berlin: Springer-Verlag. pp. 268-317. https://doi.org/10.1007/978-3-642-69759-3_9

Crosta, G.B., Frattini, P. 2004. Controls on modern alluvial fan processes in the Central Alps, Northern Italy. Earth Surface Processes and Landforms 29, 267-293. https://doi.org/10.1002/esp.1009

D'Agustino, V., 2013. Assessment of past torrential events through historical sources. In Schneuwly-Bollschweiler, M., Stoffel, M., Rudolf-Miklau, F., (Eds.) Dating Torrential Processes on Fans and Cones. Springer, Dordrecht. pp. 131-146. https://doi.org/10.1007/978-94-007-4336-6_8

Dahl, S., Nesje A., 1996. A new approach to calculating Holocene winter precipitation by combining glacier equilibrium-line altitudes and pine-tree limits: a case study from Hardangerjøkulen, central southern Norway. The Holocene 6, 381-398. https://doi.org/10.1177/095968369600600401

Dahl, S.O., Nesje, A., Lie, Ø., Fjordheim, K., Matthews, J.A., 2002. Timing, equilibrium-line altitudes and climatic implications of two early-Holocene glaciers readvances during the Erdalen Event at Jostedalsbreen, western Norway. The Holocene 12, 17-25. https://doi.org/10.1191/0959683602hl516rp

De Haas, T., Densmore, A.L., Stoffel, M., Suwa, H., Imaizumi, F., Ballesteros-Cánovas, J.A., Wasklewicz, T. 2018. Avulsions and the spatio-temporal evolution of debris-flow fans. Earth Science Reviews 177, 53-75.

https://doi.org/10.1016/j.earscirev.2017.11.007

de Moor, J. J. W., Verstraeten, G., 2008. Alluvial and colluvial sediment storage in the Geul River catchment (The Netherlands) - Combining field and modelling data to construct a Late Holocene sediment budget. Geomorphology 95, 487-503. https://doi.org/10.1016/j.geomorph.2007.07.012

Dunai, T.J., 2010. Cosmogenic Nuclides: Principles, Concepts and Applications in the Earth Surface Sciences. Cambridge: Cambridge University Press. https://doi.org/10.1017/CBO9780511804519

Eldevik, T., Risebrobakken, B., Bjune, A.E., Andersson, C., Birks, H.J.B., Dokken, T.M., Drange, H., Glessmer, M.S., Li, C., Nilsen, J.E.Ø., Ottera, O.H., Richter, K., Skagseth, Ø., 2014. A brief history of climate - the northern seas from the Last Glacial Maximum to global warming. Quaternary Science Reviews 106, 225-246. https://doi.org/10.1016/j.quascirev.2014.06.028

Ellis, S., 1979. The identification of some Norwegian mountain soil types. Norsk Geografisk Tidsskrift 33, 205-212. https://doi.org/10.1080/00291957908552055

Ellis, S., 1980. Soil-environmental relationships in the Okstindan Mountains, north Norway. Norsk Geografisk Tidsskrift 34, 167-176. https://doi.org/10.1080/00291958008621911

Førland, E.J., 1993. Nedbørnormaler, Normalperiode 1961-1990. Den Norske Meterorologiske Institutt, Oslo (Rapport 39/93).

Germain, D., Ouellet, M.A., 2014. Subaerial sediment-water flows on hillslopes: essential research questions and classification challenges. Progress in Physical Geography 37, 813-833. https://doi.org/10.1177/0309133313507943

Giles, P.T., Nichols, G.J., Wilford, D.J., (Eds.) 2010. Alluvial fans: from reconstructing past environments to identifying contemporary hazards. Geomorphology 115 (3-4). [Special Issue]

Grove J.M., Battagel, A., 1989. The rains of December 1743 in western Nor¬way. Norsk Geografisk Tidsskrift 43, 215-220. https://doi.org/10.1080/00291958908552237

Harvey, A.M., 2004. Alluvial fan. In Goudie, A.S. (Ed.) Encyclopaedia of Geomorphology, Volume 1, 15-19. Routledge, London.

Harvey, A.M., 2012. The coupling status of alluvial fans and debris cones: a review and synthesis. Earth Surface Processes and Landforms 37, 64-76. https://doi.org/10.1002/esp.2213

Harvey, A.M., 2013. Processes of sediment supply to alluvial fans and debris cones. In Schneuwly-Bollschweiler, M., Stoffel, M., Rudolf-Miklau, F., (Eds.) Dating Torrential Processes on Fans and Cones. Springer, Dordrecht. pp. 15-32. https://doi.org/10.1007/978-94-007-4336-6_2

Harvey, A.M., Mather, A.E., Stokes, M., 2005. Alluvial fans: geomorphology, sedimentology, dynamics - introduction. A review of alluvial-fan research. In: Harvey, A.M., Mather, A.E., Stokes, M., (Eds.), Alluvial Fans: Geomorphology, Sedimentology, Dynamics. Geological Society of London, Special Publication 251, 1-7. https://doi.org/10.1144/GSL.SP.2005.251.01.01

Hornung, J., Pflanz, D., Hechler, A., Beer, A., Hinderer, M., Maisch, M., Bieg, U., 2010. 3-D architecture, depositional patterns and climate triggered sediment fluxes of an alpine alluvial fan (Samedan, Switzerland). Geomorphology 115, 202-214. https://doi.org/10.1016/j.geomorph.2009.09.001.

Hughes, A.L.C., Gyllencreutz, R., Lohne, Ø., Mangerud, J., Svendsen, J.L., 2016. The last Eurasian ice sheets - a chronological database and time-slice reconstruction. Boreas 45, 1-45. https://doi.org/10.1111/bor.12142

Hungr, O., Evans, S.G., Bovis, M.J., Hutchinson, J.N., 2001. A review of the classification of landslides of the flow type. Environmental and Engineering Geoscience 7, 221-238. https://doi.org/10.2113/gseegeosci.7.3.221

Innes, J.L., 1985a. Lichenometry. Progress in Physical Geography 9, 187-254. https://doi.org/10.1177/030913338500900202

Innes, J.L., 1985b. Lichenometric dating of debris-flow deposits on alpine colluvial fans in southwest Norway. Earth Surface Processes and Landforms 10, 519-524. https://doi.org/10.1002/esp.3290100510

Innes, J.L., 1985c. Magnitude and frequency relations of debris-flows in north-west Europe. Geografiska Annaler, Series A (Physical Geography) 87A, 17-36.

Ivy-Ochs, S., Duhnforth, M., Densmore, A.L., Alfimov, V., 2013. Dating fan deposits with cosmogenic nuclides. In Schneuwly-Bollschweiler, M., Stoffel, M., Rudolf-Miklau, F., (Eds.) Dating Torrential Processes on Fans and Cones. Springer, Dordrecht. pp. 243-263. https://doi.org/10.1007/978-94-007-4336-6_16

Jansen, E., Andersson, C., Moros, M., Nisancioglu, K.H., Nyland, B.F., Telford, R.J., 2008. The early to mid-Holocene thermal optimum in the North Atlantic. In Battarbee, R.W., Binney, H.A., (Eds.) Natural Climate Variability and Global Warming: a Holocene Perspective. Wiley-Blackwell, Chichester. pp. 128-137

Jarman, D., Agliardi, F., Crosta, G.B. 2011. Megafans and outsize fans from catastrophic slope failures in Alpine glacial troughs: the Malser Haide and the Val Venosta cluster, Italy. Geological Society London Special Publications 351, 253-277. https://doi.org/10.1144/SP351.14

Jomelli, V., 2013. Lichenometric dating of debris avalanche deposits with an example from the French Alps. In Schneuwly-Bollschweiler, M., Stoffel, M., Rudolf-Miklau, F., (Eds.) Dating Torrential Processes on Fans and Cones. Springer, Dordrecht. pp. 211-224. https://doi.org/10.1007/978-94-007-4336-6_14

Kjær, K.H., Sultan, L., Krüger, J., Schomacker, A., 2004. Architecture and sedimentation of outwash fans in front of the Mýrdalsjökull ice cap, Iceland. Sedimentary Geology 172, 139-163. https://doi.org/10.1016/j.sedgeo.2004.08.002

Lal, D., 1991. Cosmic ray labeling of erosion surfaces: In situ nuclide production rates and erosion models. Earth and Planetary Science Letters 104, 424-439. https://doi.org/10.1016/0012-821X(91)90220-C

Lang, A., 2013. Luminescence dating of alluvial fans and cones. In Schneuwly-Bollschweiler, M., Stoffel, M., Rudolf-Miklau, F., (Eds.) Dating Torrential Processes on Fans and Cones. Springer, Dordrecht. pp. 283-295. https://doi.org/10.1007/978-94-007-4336-6_18

Lewis, S.G., Birnie, J.F., 2001. Little Ice Age alluvial fan development in Langedalen, western Norway. Geografiska Annaler 83A, 179-190. https://doi.org/10.1111/1468-0459.00153

Lilleøren, K.S., Etzelmüller, B., Schuler, T.V., Ginås, K., Humlum, O., 2012. The relative age of permafrost - estimation of Holocene permafrost limits in Norway. Global and Planetary Change 92-93, 209-223 https://doi.org/10.1016/j.gloplacha.2012.05.016

Lutro,O., Tveten, E., 1996. Geologiske kart over Norge, bergrunnskart Ardal, 1:250,000. Norges Geologiske Undersøkelse, Trondheim.

Matthews, J.A., 1974. Families of lichenometric dating curves from the Storbreen gletschervorfeld, Jotunheimen, Norway. Norsk Geografisk Tidsskrift 28, 215-235. https://doi.org/10.1080/00291957408551968

Matthews, J.A., 1985. Radiocarbon dating of buried soils: principles, problems and prospects. In: Richards, K.S., Arnett, R.R., Ellis, S., (Eds.) Geomorphology and Soils. George Allen and Unwin, London. pp. 269-288.

Matthews, J.A., 1991. The late Neoglacial ('Little Ice Age') glacier maximum in southern Norway: new 14C-dating evidence and climatic implications. The Holocene 1, 219-233. https://doi.org/10.1177/095968369100100304

Matthews, J.A., 2005. 'Little Ice Age' glacier variations in Jotunheimen, southern Norway: a study in regionally-controlled lichenometric dating of recessional moraines with implications for climate and lichen growth rates. The Holocene 15, 1-19. https://doi.org/10.1191/0959683605hl779rp

Matthews, J.A., Briffa, K.R., 2005. The 'Little Ice Age': re-evaluation of an evolving concept. Geografiska Annaler, Series A (Physical Geography) 87A, 17-36. https://doi.org/10.1111/j.0435-3676.2005.00242.x

Matthews, J.A., Dresser, P.Q., 2008. Holocene glacier variation chronology of the Smørstabbtindan massif, Jotunheimen, southern Norway, and the recognition of century- to millennial-scale European Neoglacial Events. The Holocene 18, 181-201. https://doi.org/10.1177/0959683607085608

Matthews, J.A., McEwen L.J., 2013. High-precision Schmidt-hammer exposure-age dating (SHD) of flood berms, Vetlestølsdalen, alpine southern Norway: first application and some methodological issues. Geografiska Annaler, Series A Physical Geography) 95A, 185-195. https://doi.org/10.1111/geoa.12009

Matthews, J.A., Owen G., 2010. Schmidt hammer exposure-age dating: developing linear age-calibration curves using Holocene bedrock surfaces from the Jotunheimen-Jostedalsbreen regions of southern Norway. Boreas 39, 105-115. https://doi.org/10.1111/j.1502-3885.2009.00107.x

Matthews, J.A., Trenbirth H.E., 2011. Growth rate of a very large crustose lichen (Rhizocarpon subgenus) and its implications for lichenometry. Geografiska Annaler, Series A Physical Geography) 93A, 27-39. https://doi.org/10.1111/j.1468-0459.2011.00004.x

Matthews, J.A., Winkler S., 2011. Schmidt-hammer exposure-age dating (SHD): application to early Holocene moraines and a reappraisal of terrestrial cosmogenic-nuclide dating TCND) at Austanbotnbreen, Jotunheimen, Norway. Boreas 40, 256-270. https://doi.org/10.1111/j.1502-3885.2010.00178.x

Matthews, J.A., Berrisford, M.S., Dresser, P.Q., Nesje, A., Dahl, S.O., Bjune, A.E., Bakke, J., Birks, H.J.B., Lie, Ø., Dumayne-Peaty, L., Barnett, C., 2005. Holocene glacier history of Bjørnbreen and climatic reconstruction in central Jotunheimen, Norway, based on proximal glaciofluvial stream-bank mires. Quaternary Science Reviews 24, 67-90. https://doi.org/10.1016/j.quascirev.2004.07.003

Matthews, J.A., Shakesby, R.A., Fabel, D., 2007. Very low inheritance in cosmogenic surface exposure ages of glacial deposits: a field experiment from two Norwegian glacier forelands. The Holocene 27, 1406-1404. https://doi.org/10.1177/0959683616687387

Matthews, J.A., McEwen, L.J., Owen, G., 2015. Schmidt-hammer exposure-age dating (SHD) of snow-avalanche impact ramparts in southern Norway: approaches, results and implications for landform age, dynamics and development. Earth Surface Processes and Landforms 40, 1705-1718. https://doi.org/10.1002/esp.3746

Matthews, J.A., Winkler, S., Wilson, P., Tomkins, M.D., Dortsch, J.M., Mourne, R.W., Hill, J.L., Owen, G., Vater, A.E., 2018. Small rock-slope failures conditioned by Holocene permafrost degradation: a new approach and conceptual model based on Schmidt-hammer exposure-age dating, Jotunheimen, southern Norway. Boreas 47, 1144-1169. https://doi.org/10.1111/bor.12336

McCarroll, D., 1987. The Schmidt hammer in geomorphology: Five sources of instrument error. British Geomorphological Research group, Technical Bulletin 36, 16-27.

McCarroll, D., 1994. The Schmidt hammer as a measure of the degree of rock surface weathering and terrain age. In Beck C. (Ed.) Dating in Exposed and Surface Contexts. University of New Mexico Press, Albuquerque. pp. 29-46.

McEwen, L.J., Matthews, J.A., 2013. Sensitivity, persistence and resolution of the geomorphological record of valley-floor floods in an alpine glacier-fed catchment, Leirdalen, Jotunheimen, southern-Norway. The Holocene 23, 974-989. https://doi.org/10.1177/0959683612475144

McEwen, L.J., Matthews, J.A., Shakesby, R.A., Berrisford, M.S., 2002. Holocene gorge excavation linked to boulder fan formation and frost weathering in a Norwegian alpine periglacio-fluvial system. Arctic, Antarctic and Alpine Research 34, 345-357. https://doi.org/10.1080/15230430.2002.12003503

McEwen, L.J., Owen, G., Matthews, J.A., Hiemstra, J., 2011. Late-Holocene development of a Norwegian alpine alluvial fan affected by cyclical distal undercutting, proximal glacier variations and episodic snow-avalanche activity. Geomorphology 127, 198-21. https://doi.org/10.1016/j.geomorph.2010.12.016

Mercier, D., 2008. Paraglacial and paraperiglacial landsystems: concepts, temporal scales and spatial distribution. Géomorphologie 14, 223-233. https://doi.org/10.4000/geomorphologie.7396

Moen, A., 1999. National Atlas of Norway: Vegetation. Norwegian Mapping Authority, Hønefoss.

Nesje, A., 2009. Latest Pleistocene and Holocene alpine glacier fluctuations in Scandinavia. Quaternary Science Reviews 28, 2119-2136. https://doi.org/10.1016/j.quascirev.2008.12.016

NIJOS, 1991. Vegetasjonskart: Galdhøpiggen 1518 II (1:50,000). Norsk institutt for jordog skogkartlegging (NIJOS), Ås.

Parker, G., Paola, C., Whipple, K.X., Mohrig, D., 1998. Alluvial fans formed by channelized fluvial and sheet flow. Journal of Hydraulic Engineering 124, 985-995. https://doi.org/10.1061/(ASCE)0733-9429(1998)124:10(985)

Pierson, T.C., 2005. Hyperconcentrated flow - transitional process between water flow and debris flow. In Jakob, M., Hungr. O., (Eds.) Debris Flows/Avalanches. Geological Society of America, 1-12.

Poulos, M., Pierce, J., 2018. Alluvial fan depositional records from north and south-facing catchments in semi-arid montane terrain. Quaternary Research 89, 237-253. https://doi.org/10.1017/qua.2017.98

Powers, M.C., 1953. A new roundness scale for sedimentary particles. Journal of Sedimentary Petrology 23, 117-119. https://doi.org/10.1306/D4269567-2B26-11D7-8648000102C1865D

Proceq, 2004: Operating instructions. Betonprüfhammer N/NR-L/LR. Proceq SA, Schwerzenbach.

Rachocki, A.H., Church, M., 1990. Alluvial fans - a Field Approach. Wiley, Chichester.

Roald L.A., 2000. The large flood of 1860 in Norway. In: Snorrason A, Finnsdottir HP , Moss ME (Eds.) The Extreme of the Extremes: Extraor¬dinary Floods. IAHS Publication no. 271, pp. 173-178.

Roald L.A., 2003. Two major 18th century flood disasters in Norway. In:Thorndycraft R, Benito G, Barriendos M et al., (Eds.) Palaeofloods, Historical Data and Climatic Variability: Applications in Flood Risk Assessment. Proceedings of the International PHEFRA Workshop, Barcelona, Spain, October 2002, pp. 125-130.

Scheinert, C., Wasklewicz, T., Staley, D., 2012. Alluvial Fan Dynamics - Revisiting the Field Geography Compass 6/12, 752-775. https://doi.org/10.1111/gec3.12004

Schneuwly-Bollschweiler, M., Stoffel, M., Rudolf-Miklau, F., 2013. Dating torrential processes on fans and cones. Springer, Dordrecht. https://doi.org/10.1007/978-94-007-4336-6

Seppä, H., Bjune, A.E, Telford, R.J., Birks, H.J.B., Birks, H.H., Veski, S., 2009. Last nine-thousand years of temperature variability in Northern Europe. Climate Past 5, 523-535. https://doi.org/10.5194/cp-5-523-2009

Shakesby, R.A., Matthews, J.A., Karlén, W., Los, S., 2011. The Schmidt hammer as a Holocene calibrated-age dating technique: testing the form of the R-value - age relationship and defining predicted errors. The Holocene 21, 615-620. https://doi.org/10.1177/0959683610391322

Stahl, T., Winkler, S., Quigley, M., Bbbington, M., Duffy, B., Duke, D., 2013. Schmidt hammer exposure-age dating (SHD) of late Quaternary fluvial terraces in New Zealand. Earth Surface Processes and Landforms 38, 1838-1850. https://doi.org/10.1002/esp.3427

Stock, J.D., 2013. Waters divided: a history of alluvial fan research and a view of its future. In Wohl, E., (Ed.) Treatise on Geomorphology, Volume 9, Fluvial Geomorphology. Academic Press-Elsevier, Amsterdam. pp. 413-458. https://doi.org/10.1016/B978-0-12-374739-6.00249-9

Stoffel, M., 2013. Tree-ring record of debris-flow dynamics and triggering rain storms in Ritigraben (Swiss Alps) since AD 1570. In Schneuwly-Bollschweiler, M., Stoffel, M., Rudolf-Miklau, F., (Eds.) Dating Torrential Processes on Fans and Cones. Dordrecht: Springer, 211-224. https://doi.org/10.1007/978-94-007-4336-6_11

Stone, J., 2000. Air pressure and cosmogenic isotope production. Journal of Geophysical Research 105, 23753-23760. https://doi.org/10.1029/2000JB900181

Støren, E.N., Paasche, O., 2014. Scandinavian floods: From past observations to future trends. Global and Planetary Change 113, 34-43. https://doi.org/10.1016/j.gloplacha.2013.12.002

Stroeven, A.P., Hättestrand, C., Kleman, J., Heiman, J., Fabel, D., Fredin, O., Good fellow, B.W., Harbor, J.M., Jansen, J.D., Olsen, L., Caffee, M.W., Fink, D., Sundqvist, J., Rosqvist, G.C., Stromberg, B., Janson, K.N., 2016. Deglaciation of Fennoscandia. Quaternary Science Reviews 147, 91-121. https://doi.org/10.1016/j.quascirev.2015.09.016

Tomkins, M.D., Dortch, J.M., Hughes, P.D., 2016: Schmidt hammer exposure dating (SHED): establishment and implications for the retreat of the last British Ice Sheet. Quaternary Geochronology 33, 46-60. https://doi.org/10.1016/j.quageo.2016.02.002

Tomkins, M.D., Dortch, J. M., Hughes, P.D., Huck, J.J., Stimson, A.G., Delmas, M., Calvet, M., Pallàs, R. 2018. Schmidt hammer exposure dating (SHED): rapid age assessment of glacial landforms in the Pyrenees. Quaternary Research 90, 26-37. https://doi.org/10.1017/qua.2018.12

Velle, G., Bjune, A.E., Larsen, J., Birks, H.J.B., 2010. Holocene climate and environmental history of Brurskardstjørni, a lake in the catchment of Øvre Heimdalsvatnet, south-central Norway. Hydrobiologia 642, 13-34. https://doi.org/10.1007/s10750-010-0153-7

Ventra, D., Clarke, L.E., (Eds.) 2018. Geology and geomorphology of alluvial and fluvial fans. Geological Society of London, Special Publications 440, 1-21. https://doi.org/10.1144/SP440.16

Wells S.G., Harvey, A.M., 1987. Sedimentologic and geomorphic variations in storm generated alluvial fans, Howgill Fells, northwest England. Geological Society of America Bulletin 98, 182-198. https://doi.org/10.1130/0016-7606(1987)98<182:SAGVIS>2.0.CO;2

Wilford, D.J., Sakals, M.E., Innes, J.L., Sidle, R.C., Bergerud, W.A., 2004. Recognition of debris flow, debris flood and flood hazard through watershed morphometrics. Landslides 1, 61-66. https://doi.org/10.1007/s10346-003-0002-0

Wilford, D.J., Sakals, M.E., Innes, J.L., Sidle, R.C., 2005. Fans with forests: contemporary hydrogeomorphic processes on fans with forests in west-central British Columbia, Canada. In: Harvey, A.M., Mather, A.E., Stokes, M., (Eds.), Alluvial Fans: Geomorphology, Sedimentology, Dynamics. Geological Society of London, Special Publication 251, 25-40. https://doi.org/10.1144/GSL.SP.2005.251.01.03

Williams, G., 1983. Paleohydrological methods and some examples from Swedish fluvial environments: I. Cobble and boulder deposits. Geografiska Annaler Series A 65A, 224-243. https://doi.org/10.1080/04353676.1983.11880088

Wilson, P., Matthews, J.A., 2016. Age assessment and implications of late Quaternary periglacial and paraglacial landforms on Muckish Mountain, northwest Ireland, based on Schmidt-hammer exposure-age dating (SHD). Geomorphology 270, 134-144. https://doi.org/10.1016/j.geomorph.2016.07.002

Wilson, P., Matthews, J.A., Mourne, R.W., 2017. Relict blockstreams at Insteheia, Valldalen-Tafjorden, southern Norway: their nature and Schmidt-hammer exposure age. Permafrost and Periglacial Processes 28, 286-297. https://doi.org/10.1002/ppp.1915

Wilson, P., Linge, H., Matthews, J.A., Mourne, R.W., Olsen, J., 2019: Comparative numerical surface-age dating (10Be and Schmidt hammer) of an early-Holocene rock avalanche at Alnesfjellet, Valldalen, southern Norway. Geografiska Annaler Series A, Physical Geography 101, 293-309. https://doi.org/10.1080/04353676.2019.1644815

Winkler, S., Matthews, J.A., Mourne, RW., Wilson, P., 2016:Schmidt hammer exposure ages from periglacial patterned ground (sorted circles) in Jotunheimen, Norway, and their interpretive problems. Geografiska Annaler Series A, Physical Geography 98, 265-285. https://doi.org/10.1111/geoa.12134

List of Figures

Fig. 1	The drainage basin of the Ytre Illåe in relation to the Illåe fan, showing contributing glaciers, and maximum glacial extents during the Little Ice Age.
Fig. 2	Aerial photograph of the Illåe fan with mapped outlines of the upper fan surface (solid line), terrace areas (dashed line, T) and SHD sampling zones (dotted line): X = location of TCND sample in zone 5; I = inset fan; G = bedrock gorge of the Ytre Illåe at the fan apex; L = confluence with the Leira; H = outwash fan of the Hurra (glacial river from Hurrbrean). Note also the elongated boulder deposits and dendritic channel network on the upper fan surface (photo from http://www.norgeibilder.no)
Fig. 3	(A) Location of TCND site within zone 5 of the upper fan surface (the figure is standing on the sampled boulder at the distal end of the boulder deposit). (B) *In situ* sampled quartzitic boulder. Note the lichen cover and large size of yellow-green crustose lichens on the boulders.
Fig. 4	The sequence of four terraces to the south of the Ytre Illåe within the entrenched Illåe fan
Fig. 5	Surface features of the Illåe fan: (A-C) boulder deposits and channels on the upper fan surface; (D) boulder deposits and channels on surface of the inset fan
Fig. 6	Boulder characteristics from the upper fan surface: (A) parameters summarising boulder size; (B) histograms of boulder roundness with mean roundness values for each sample
Fig. 7	Entrenchment and internal structure and stratigraphy of the Illåe fan: (A) entrenched proximal fan (north-side), upper fan surface close to the fan apex, and bedrock-controlled channel; (B) distal part of the entrenched fan and proximal edge of the inset fan (left); (C and D) fan sections (south-side)
Fig. 8	Synthetic stratigraphic section through the fan showing crude stratification with matrix-supported (MS) and clast-supported (CS) boulder-rich layers in a predominantly sand-rich matrix
Fig. 9	Soil profiles from the upper fan surface and incised terraces. See Table 4 for details of the radiocarbon dates.
Fig. 10	Conceptual model of glacially-fed alluvial fan evolution linked to Holocene environmental changes summarizing three phases of fan development: Phase 1, early-Holocene aggradation; Phase 2, mid-Holocene stability; and Phase 3 late-Holocene entrenchment.

Table 1. Clast size from boulder deposits on the upper fan surface, the inset fan, and the current active zone. Shaded zones have lowest hydraulic parameters for entrainment (D_{max}) that exceed 2m. See text for calculation of parameters.

Sampled zone	D_{50} (m)	D_{84} (m)	D_{max} (m)	D_{min} (m)	Unit stream power - ω (W m^2}	Bed shear stress -τ (N m^2)	Mean flow velocity (m s^{-1})
Zone 1 (south-side)	0.59	0.86	1.50	0.32	1063	255	2.5
Zone 2	0.85	1.25	3.20	0.60	2847	544	3.7
Zone 3	0.96	1.57	2.80	0.52	2393	476	3.4
Zone 4	0.93	1.40	3.20	0.41	2847	544	3.7
Zone 5	0.38	0.49	0.75	0.24	432	128	1.8
Zone 6 (north-side)	0.80	1.09	3.00	0.41	2617	510	3.6
Zone 7	0.67	0.81	1.20	0.42	795	204	2.3
Zone 8	0.65	0.79	0.92	0.45	563	156	2.0
Active zone (Ytre Illåe)	0.66	0.84	1.13	0.32	736	192	2.2
Inset fan	0.17	0.29	0.90	0.08	547	153	2.0

Table 2. Mean Schmidt-hammer R-values and SHD age estimates for boulder deposits from the eight zones of the upper fan surface.

Parameter	South-side					North-side		
	Zone 1	Zone 2	Zone 3	Zone 4	Zone 5	Zone 6	Zone 7	Zone 8
Mean R-value (R_s) with 95% confidence interval	47.15 ±1.00	45.15 ±0.89	45.21 ±0.82	44.1± 0.83	44.01 ±0.92	44.58 ±0.90	45.87 ±1.11	44.94 ±0.59
SHD age (years) with 95% confidence interval	7080 ±450	7805 ±425	7785 ±405	8190 ±415	8220± 440	8015 ±430	7545 ±485	7885 ±350

Table 3. Lichen sizes (largest diameter) and minimum lichenometric ages for boulder deposits on fan and terrace surfaces. Lichenometric ages were calculated using the 'Central Jotunheimen' lichenometric dating curve based on the mean of the five largest lichens (Matthews, 2005)

Fan or terrace surface	Single largest lichen (mm)	Mean of the five largest lichens (mm)	Lichenometric age (years)
Upper fan surface south-side	350	328	1764
Terrace 1 (south-side)	365	246	874
Terrace 2 (south-side)	165	85	149
Terrace 3 (south-side)	112	97	179
Terrace 4 (south-side)	68	57	92
Upper fan surface (north-side)	448	353	2163
Terrace 1 (north-side)	330	283	1208
Terrace 2 (north-side)	195	172	432
Inset fan	202	181	474

Table 4. Radiocarbon dates from soils and palaeosols

Site	Sample depth (cm)	Laboratory No.	^{14}C age +/-1σ (years)	$\delta^{13}C$ (o/oo)	Calibrated age 1 +/- 2σ	Calibrated age 2 +/- 2σ
Upper fan surface (south-side)	5-8	SWAN-1036	750+/-50	-24.7	756 (672) 571	773-646 (0.95)
Upper fan surface (south-side)	8-11	SWAN-1037	1010+/-50	-24.5	1049 (930) 791	1003-793 (0.95)
Terrace 3 (south-side)	10-11	SWAN-1038	870+/-50	-24.8	923 (784) 674	835-693 (0.72)
Upper fan surface (north-side)	17-20	SWAN-1039	1820+/-50	-23.8	1873 (1727) 1610	1874-1686 (0.87)
Terrace 1 (north-side)	41-42	SWAN-1043	470+/-50	-23.9	617 (513) 462	559-432 (0.92)

Calibration 2: 2σ age range around (in brackets) the intercept age
Calibration 2: 2σ maximum and minimum age with (in brackets) its probability

Fig 1. The drainage basin of the Ytre Illåe in relation to the Illåe fan, showing contributing glaciers, and maximum glacial extents during the Little Ice Age.

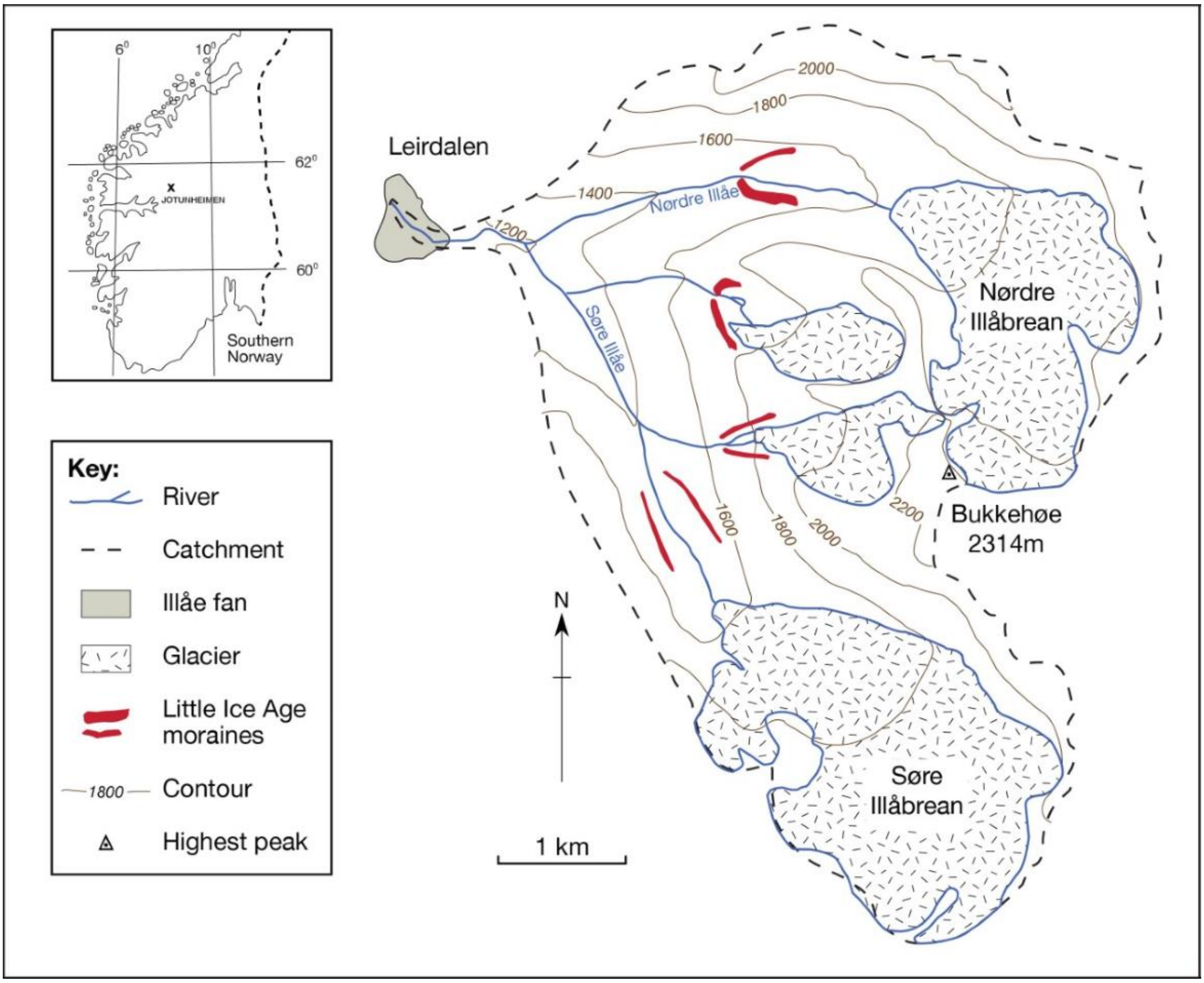

Fig 2. Aerial photograph of the Illåe fan with mapped outlines of the upper fan surface (solid line), terrace areas (dashed line, T) and SHD sampling zones (dotted line): X = location of TCND sample in zone 5; I = inset fan; G = bedrock gorge of the Ytre Illåe at the fan apex; L = confluence with the Leira; H = outwash fan of the Hurra (glacial river from Hurrbrean). Note also the elongated boulder deposits and dendritic channel network on the upper fan surface (photo from http://www.norgeibilder.no)

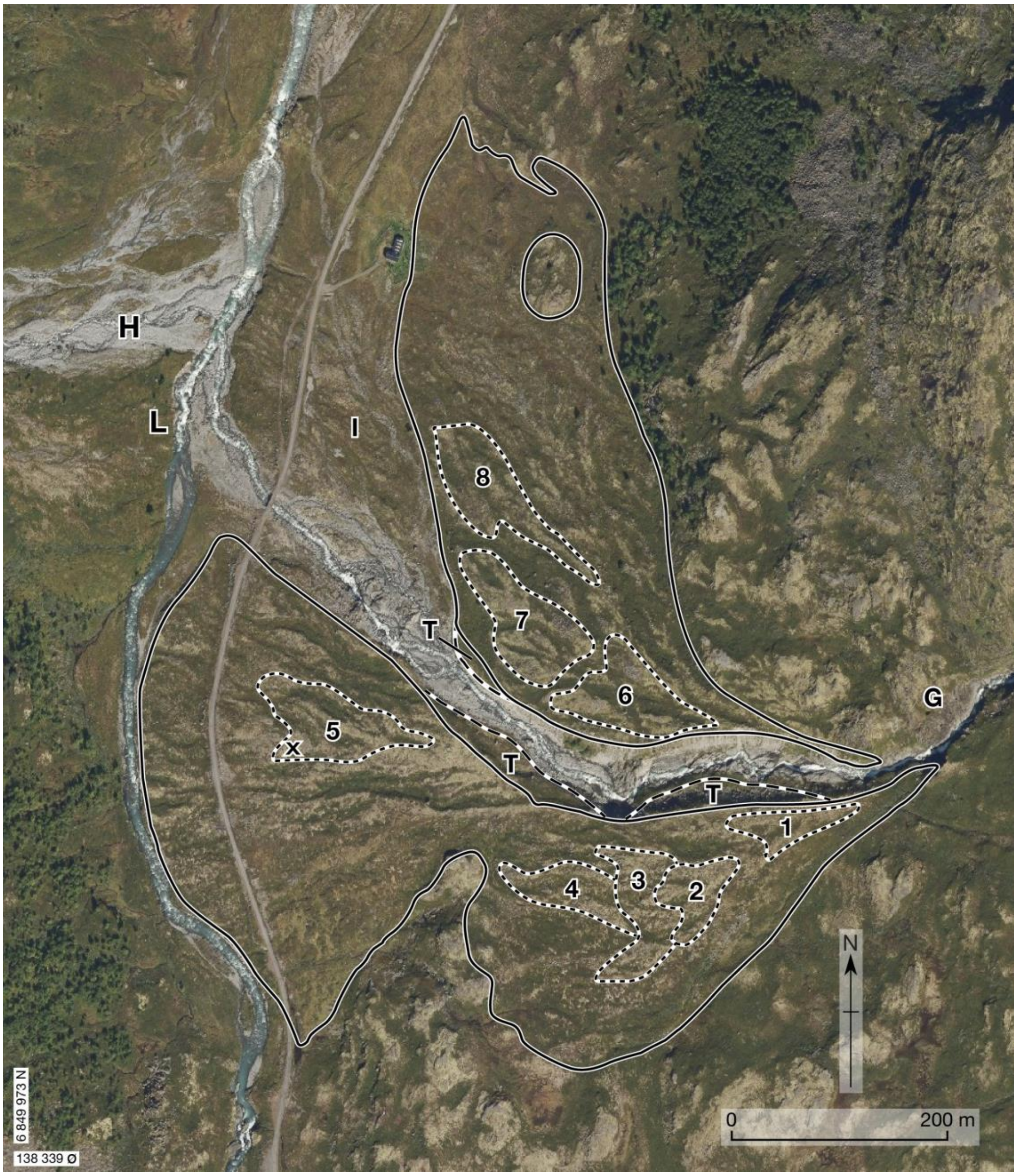

Fig 3: (A) Location of TCND site within zone 5 of the upper fan surface (the figure is standing on the sampled boulder at the distal end of the boulder deposit). (B) *in situ* sampled quartzitic boulder. Note the lichen cover and large size of yellow-green crustose lichens on the boulders.

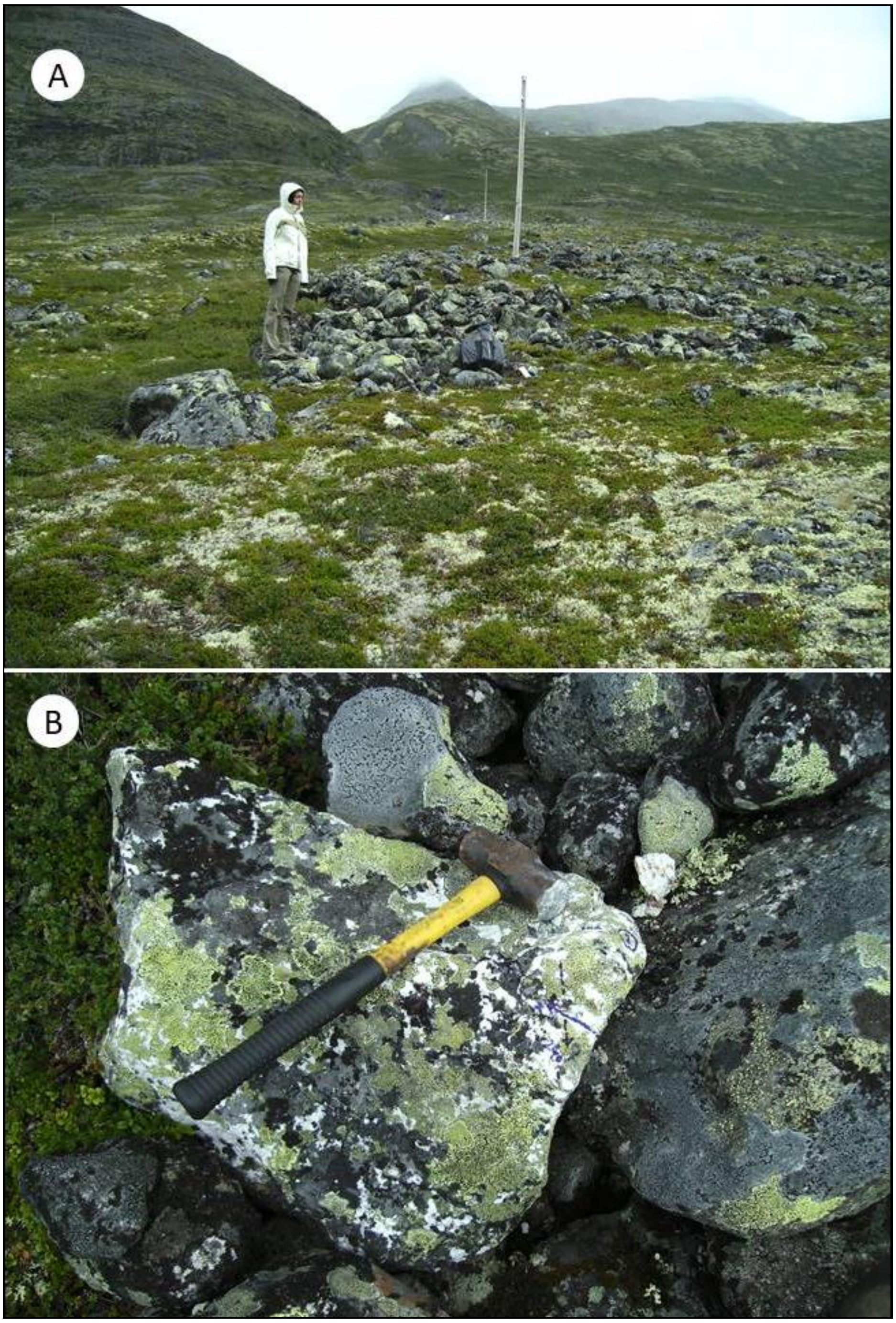

Fig. 4. The sequence of four terraces to the south of the Ytre Illåe within the entrenched Illåe fan.

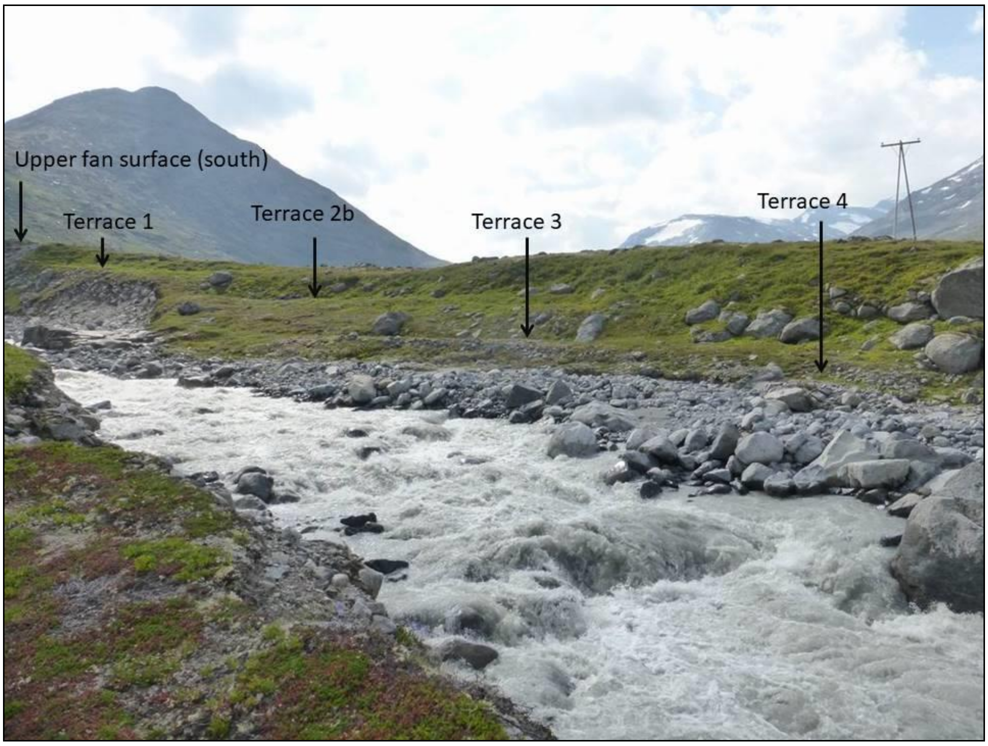

Fig. 5. Surface features of the Illåe fan: (A-C) boulder deposits and channels on the upper fan surface; (D) boulder deposits and channels on surface of the inset fan.

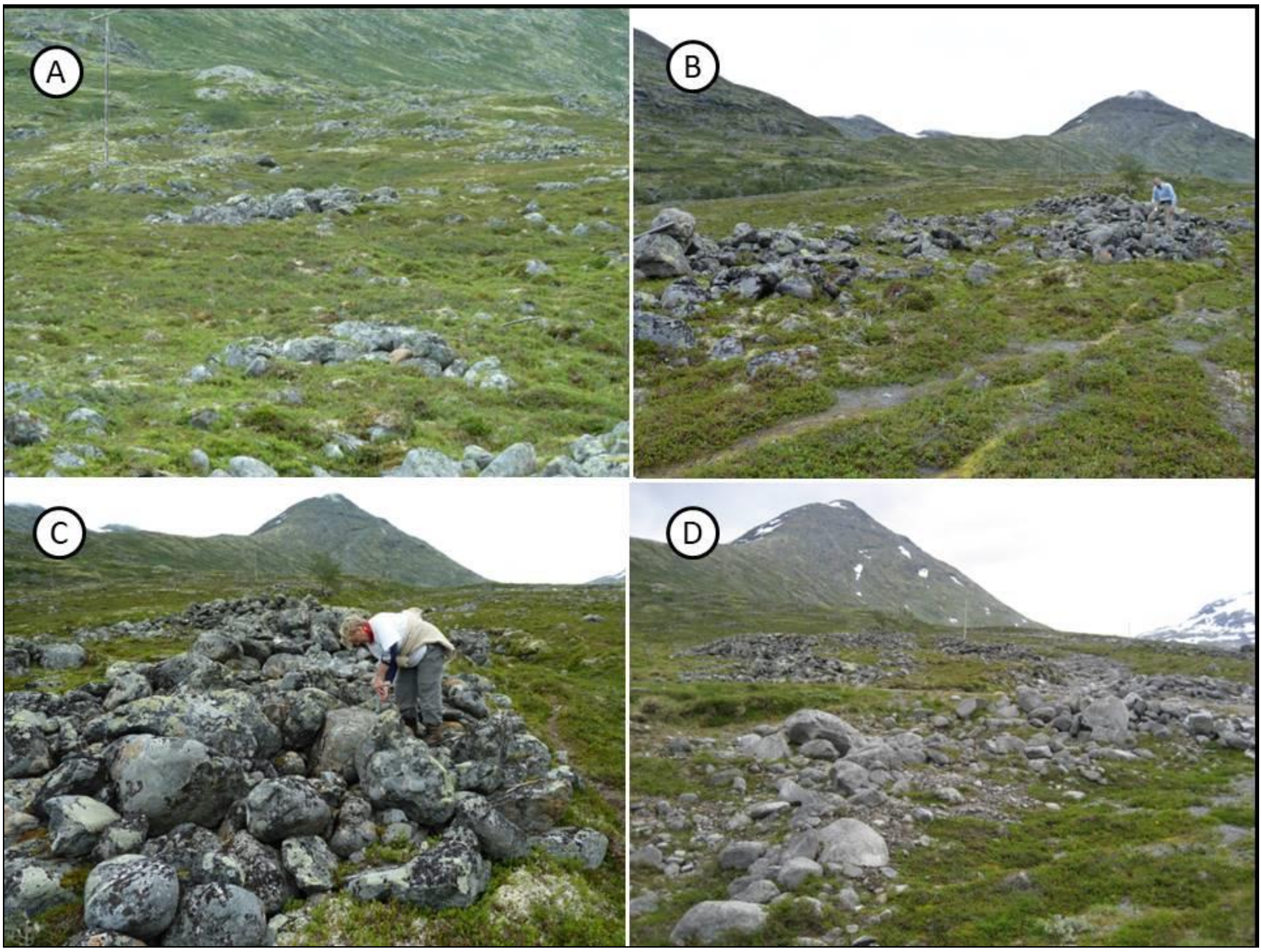

Fig. 6. Boulder characteristics from the upper fan surface: (A) parameters summarising boulder size; (B) histograms of boulder roundness with mean roundness values for each sample.

A

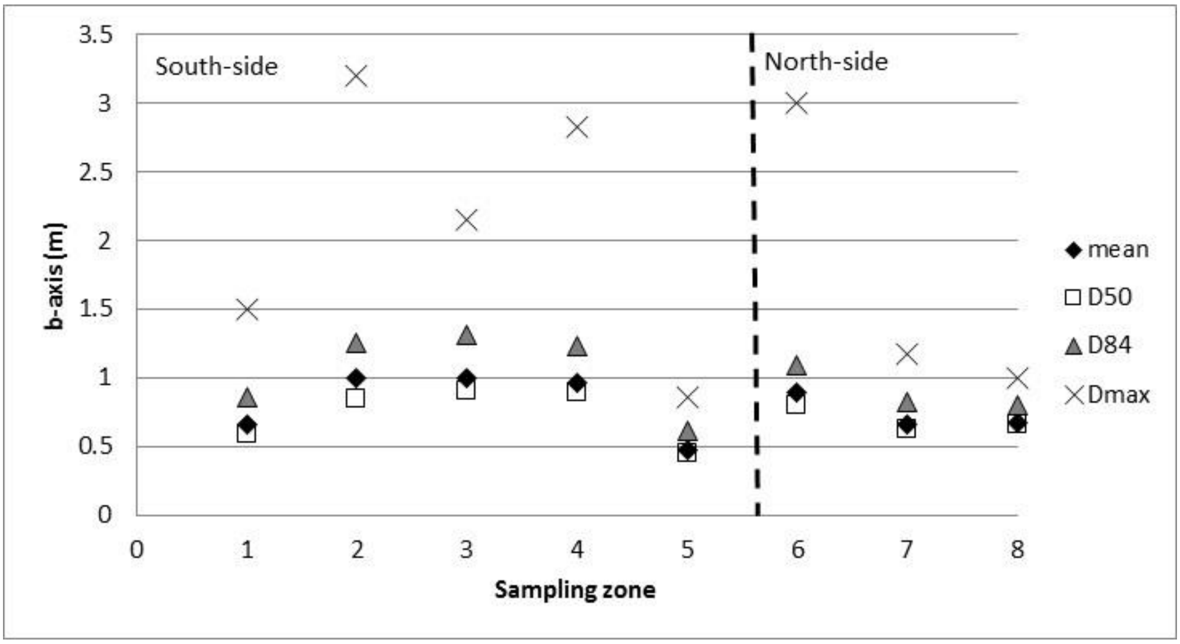

B

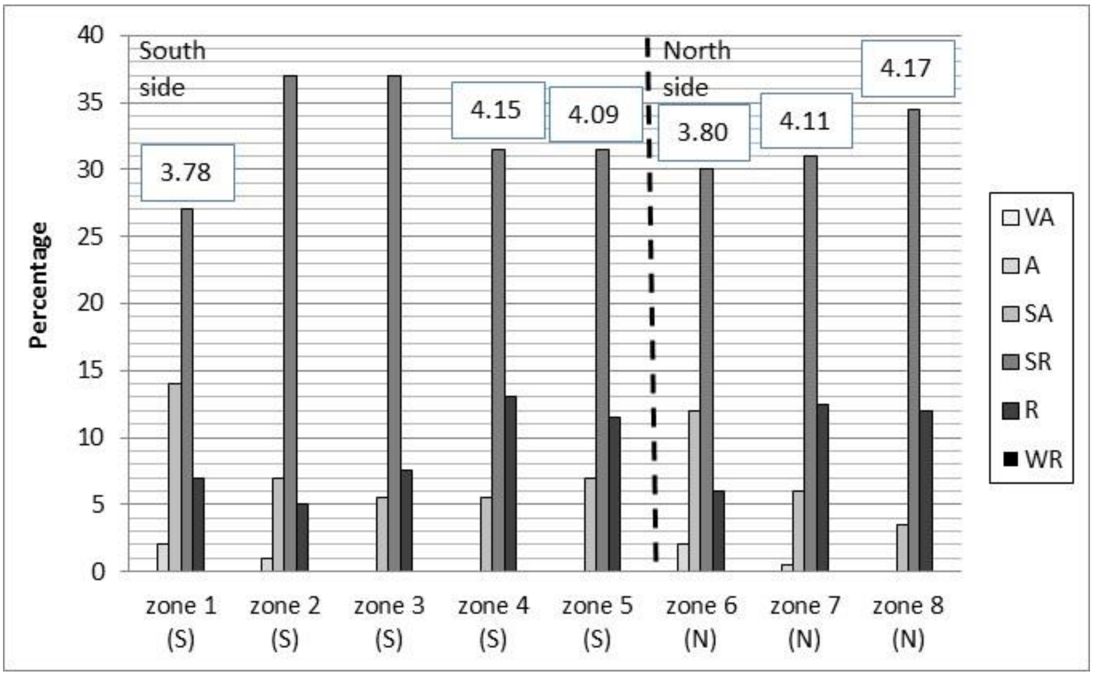

Fig 7. Entrenchment and internal structure and stratigraphy of the Illåe fan (A) entrenched proximal fan (north-side), upper fan surface close to the fan apex, and bedrock-controlled channel; (B) distal part of the entrenched fan and proximal edge of the inset fan (left); (C and D) fan sections (south-side)

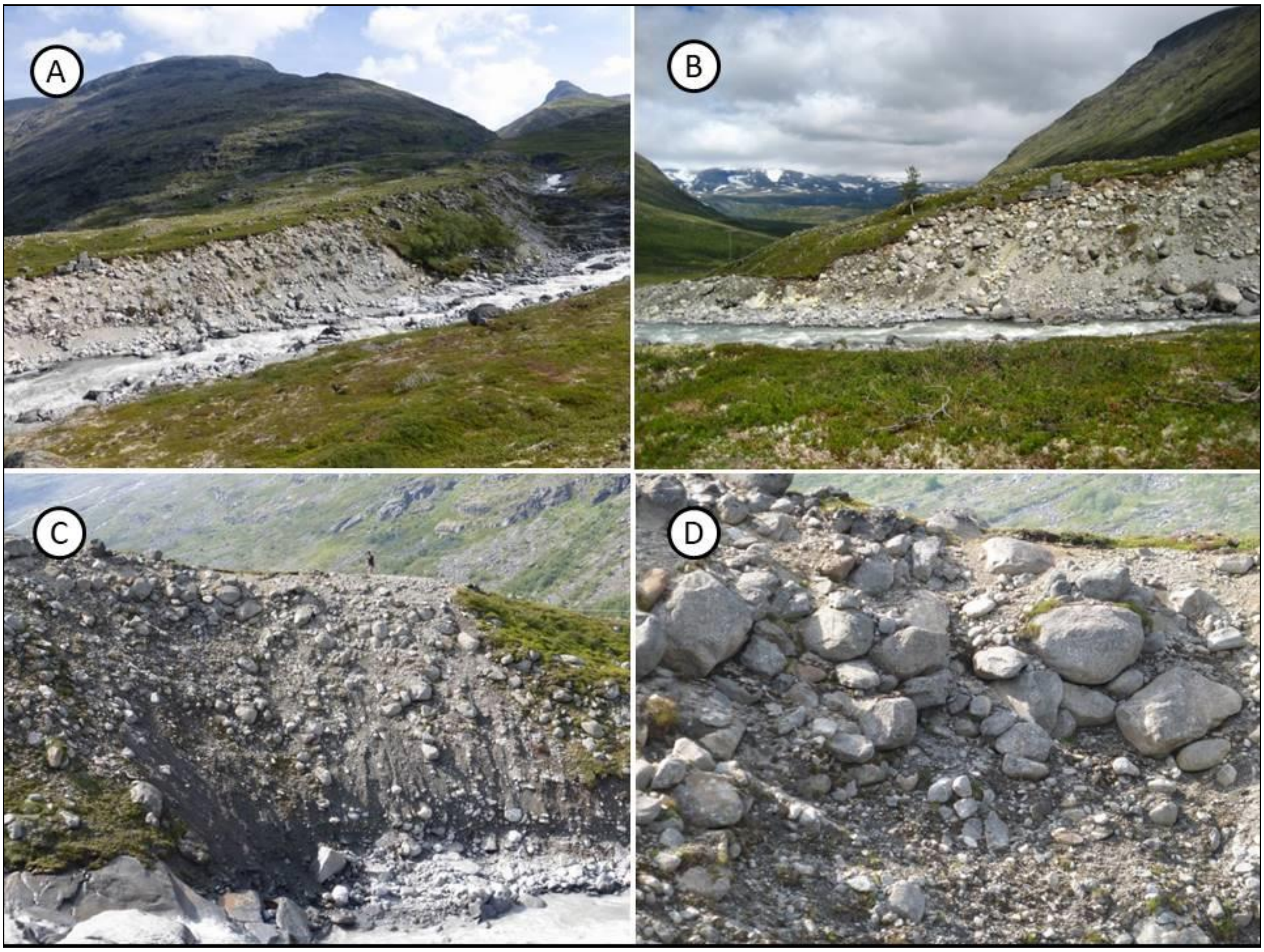

Fig. 8. Synthetic stratigraphic section through the fan showing crude stratification with matrix-supported (MS) and clast-supported (CS) boulder-rich layers in a predominantly sand-rich matrix

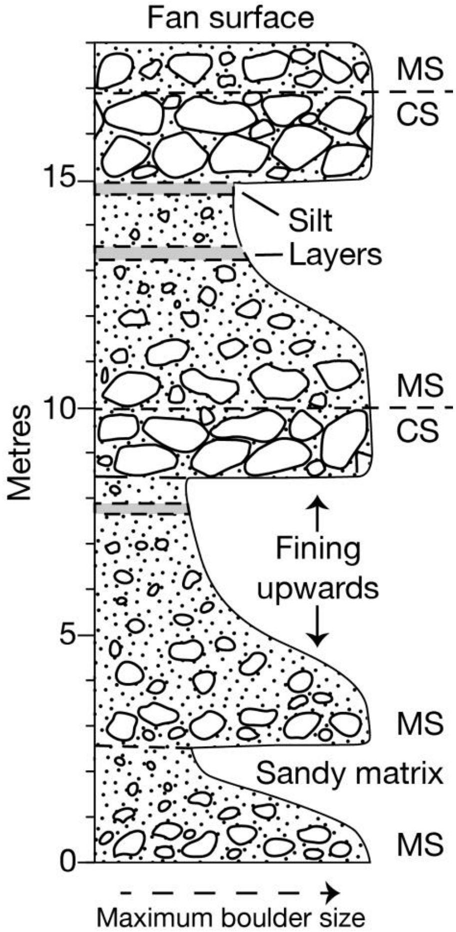

Fig. 9. Soil profiles from the upper fan surface and incised terraces. See Table 4 for details of the radiocarbon dates.

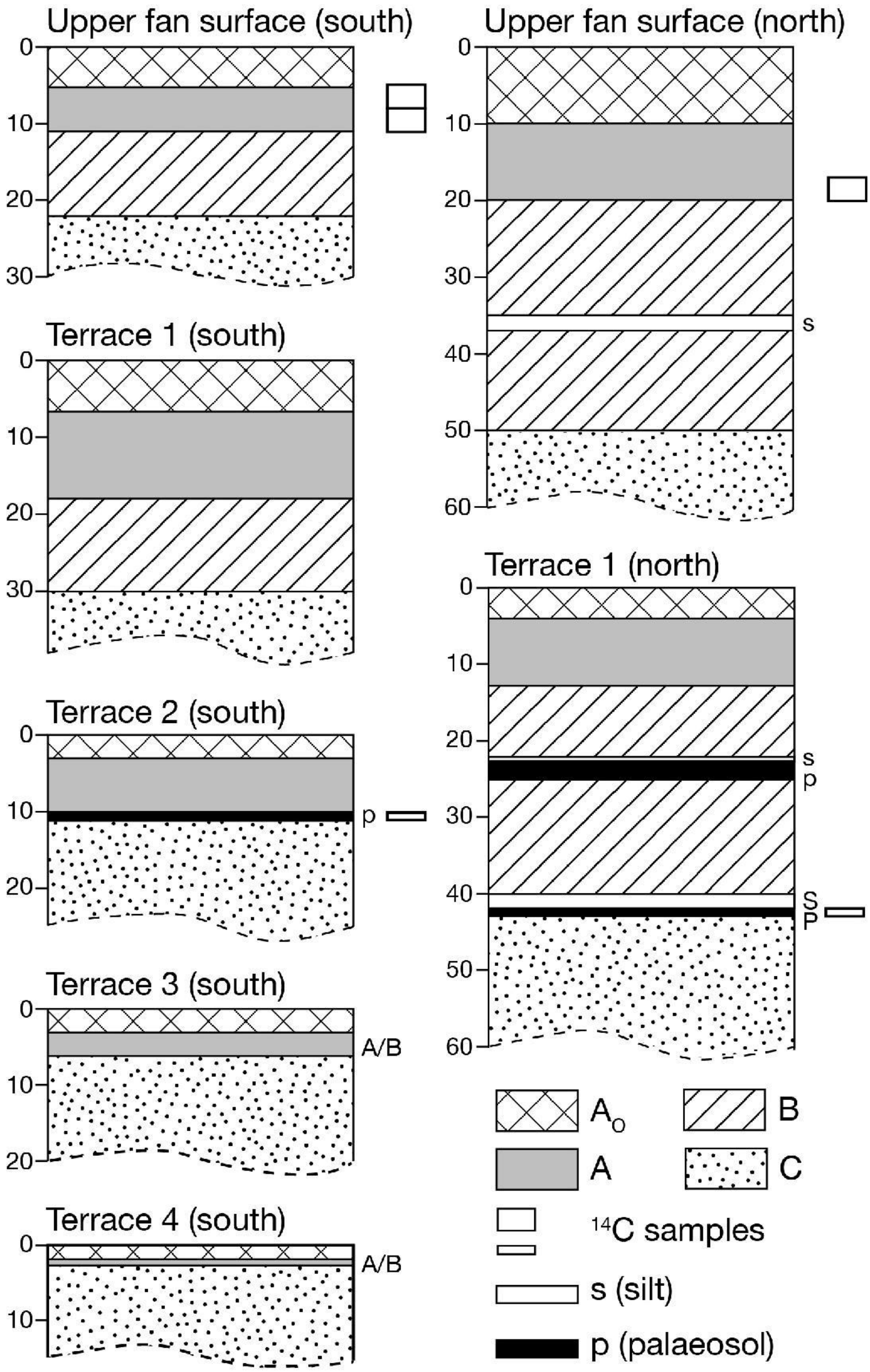

Fig. 10. Conceptual model of glacially-fed alluvial fan evolution linked to Holocene environmental changes summarizing three phases of fan development: Phase 1, early-Holocene aggradation; Phase 2, mid-Holocene stability; and Phase 3 late-Holocene entrenchment.

	Phase 1	**Phase 2**	**Phase 3**
Timing	9.7–8.0 ka (early Holocene)	8.0–5.5 ka (mid Holocene)	5.5–0 ka (late Holocene)
Climatic regime	Rapidly rising temperatures	Holocene Thermal Maximum	Cooling trend with fluctuations
State of the glaciers	Deglaciation; rapid retreat of large glaciers	Glaciers absent from the catchment	Neoglaciation: growth of small glaciers
Vegetation	Alpine plant colonisation throughout the catchment; disturbed tree cover on the fan surface	Undisturbed throughout the catchment; forested fan surface	Forest decline on the fan surface
Sediment supply	Excessive sediment supply from paraglacial sources	Drastically reduced sediment supply from the catchment	Increasing but fluctuating sediment supply
Flow type	Hyperconcentrated flow; very high sediment concentrations	Stream flow; very low sediment concentrations	Stream flow; increasing sediment concentrations
Hydrological events	High-magnitude debris floods	Largely non-erosive water floods	Increasingly erosive water floods
Geomorphodynamics	Rapid fan aggradation with boulder deposition	Stabilization of the fan surface; hiatus in sedimentation	Entrenchment, terrace formation and inset fan development